High resolution hydrogeochemical survey and estimation of baseline concentrations of trace elements in surface water of the Itacaiúnas River Basin, southeastern Amazonia: implication for environmental studies

Prafulla Kumar Sahoo[1*], Roberto Dall'Agnol[1], Gabriel Negreiros Salomão[1], Jair da Silva Ferreira Junior[1], Marcio Sousa Silva[1], Pedro Walfir Martins e Souza Filho[1], Mike A Powell[2], Rômulo Simões Angélica[3], Paulo Rógenes Pontes[1], Marlene Furtado da Costa[4], José Oswaldo Siqueira[1]

[1]Instituto Tecnológico Vale (ITV), Rua Boaventura da Silva, 955, Belém, 66055-090, PA, Brasil; [2]Independent Geologist & Pres., Geocon Environmental Consulting, London, ON, N6G3H9, Canada; [3]Instituto de Geociências (IG), Universidade Federal do Pará (UFPA), Rua Augusto Corrêa, 1, Belém, 66075-110, PA, Brasil; [4]Gerência de Meio Ambiente - Minas de Carajás, Departamento de Ferrosos Norte, Estrada Raymundo Mascarenhas, S/N Mina de N4, Parauapebas, 68516-000, PA, Brasil.

*** Corresponding author:**

Email address: prafulla.sahoo@itv.org; prafulla.iitkgp@gmail.com (P. K Sahoo)

Abstract

A high resolution (high density) survey is required to estimate site-specific baseline metal levels in water on a local scale, and is an essential part of environmental risk assessment. This methodology was used in a project in the Itacaiúnas River Basin, southeastern Amazon, which includes several mines of the Carajás Mineral Province (as part of the Itacaiúnas Geochemical Mapping and Background Project, ItacGMBP). A total of 1429 samples (including 55 duplicates) were collected in 2017 at 900 sites at one sample per microbasin, during both dry and rainy periods. The analyses of 34 elements were carried out using Inductively Coupled Plasma Mass Spectrometry (ICP-MS). In general, the waters are slightly alkaline and are classified as mixed Ca-Na-HCO_3, indicating that they are mainly influenced by silicate rock weathering. Most metal concentrations in the water are low, except Fe and Mn. Seasonality explains differences in metal concentrations, with higher values being obtained in the rainy season. Baseline threshold values (B_{TVs}) were calculated separately for both seasons by employing different statistical methods: iterative 2σ preferentially delivered the 'natural' B_{TVs} (NB_{TVs}) which is considered as the least degraded with low or no significant level of anthropogenic influence; and 98th percentile provides the 'ambient' B_{TVs} (AB_{TVs}), which consists of natural plus diffuse anthropogenic input in the defined area. The AB_{TVs} of Fe and Mn significantly exceed the WHO and CONAMA 357/05 limits. Spatial distribution indicates that Fe and Mn are not strictly related to geologic setting, rather they are highly influenced by specific local land use as well as deep weathering of the catchment and intense leaching and run-off during the rainy season. However, higher Mn occurrence in the dry period results from redox cycling of Fe and Mn via biogeochemical processes. The AB_{TVs} of Ni, Cr, and V are controlled by bedrock lithology (geologic setting), mainly associated with mafic-ultramafic rocks; Cu is associated with two large hydrothermally mineralized copper belts. The estimation of baseline levels of As, Se, and Pb were highly limited due to of the large number of samples with results less than detection limits, in this case the 95th percentile was used for their B_{TVs}. Geochemical data as well as anomalous values for most of the metals indicate that anthropogenic influence from point sources is highly negligible in the basin, except at a few points, where high NO_3 has been observed, probably due to more intense human and livestock activity. This study demonstrates that site-specific geochemical baseline assessment is a crucial factor when evaluating surficial water conditions in a large basin.

Keywords: Hydrogeochemical survey, Geochemical baseline, Heavy metals, Itacaiúnas River Basin, Southeastern Amazon, Carajás Mineral Province.

1. Introduction

Growing global concern about the protection of water quality has led to increasing attention to monitoring and risk assessment of potentially toxic metals in water bodies, however, high-resolution (or high density) hydrogeochemical studies to assess water quality are rare. High resolution surveying was introduced in the late 1960s for mineral exploration and geological mapping. This technique has evolved into an important geochemical survey for addressing a wide range of potential environmental applications, including risk assessment of toxic metals in water and soil bodies (Caritat and Cooper, 2016; Johnson et al., 2005; Labuschagne et al., 1993; Plant et al., 1997). Some regional and national hydrogeochemical high resolution surveys have been conducted on surface water bodies including a Geochemical Baseline Survey (GBASE) of North Wales stream water (Simpson et al., 1993; Simpson et al., 1996), the Forum of European Geological Survey (FOREGS) (Plant et al., 1997), the Southern River catchment survey in Australia by the Commonwealth Scientific and Industrial Research Organisation (CSIRO) (Donnet al., 2010), and regional hydrogeochemical mappings in Central Chile (Jorquera et al., 2015) and Oppdal/Berkåk, Norway (Reimann et al., 2018). One of the main advantages of using high-density surveys is the potential for determining high quality geochemical background or baseline values. This methodology provides more detailed information about the spatial variability of chemical elements in relation to the distribution of different geological units, topography, geomorphology, which allows identification of anomalous values related to mineralization, and discrimination between geogenic and anthropogenic sources (Ander et al., 2013; Caritat and Cooper, 2016; Johnson et al., 2005; Lombard et al., 1999; Pinto et al., 2014). Anthropogenic activities, such as deforestation and land use change, are considered important drivers of change in natural hydrological regimes and the consequent impact on stream water quality (Brion et al., 2011; Levy et al., 2018; Nóbrega et al., 2018; Souza-Filho et al., 2016).Significant impact has been observed after conversion of tropical forest to agriculture and cropland or pasture using this technique (Souza-Filho et al., 2016; Jacobs et al., 2017).

Water quality can be highly variable due to local lithological and environmental conditions. Identifying site-specific water quality characterization for individual watersheds is usually warranted for undertaking environmental risk assessments (Arpine and Gayane, 2016). Geochemical background, which is defined as the natural concentration range of an element in a given area, is one of the prerequisites to determine site-specific objectives for any watershed or ecosystem (Arpine and Gayane, 2016; Galuszka, 2007) and to distinguish between natural and anthropogenic origin and impact for specific elements (Gałuszka, 2007; Reimann and Garrett, 2005). This is particularly relevant when discussing the occurrence and distribution of potentially toxic heavy metals, especially when developing policy or guidelines for pollutants in

water (Gałuszka and Migaszewski, 2011; Marandi and Karro, 2008; Salminen and Tarvainen, 1997). Water quality, of which metals are important, impacts health, which translates into better education through learning ability in youth, or higher quality of life, based on less sick time, and lost wages; this is critical in developing countries. Determining natural background concentrations in water is not straightforward because of the ubiquitous anthropogenic and natural influences on water chemistry. Although a 'geochemical baseline' is sometimes used as equivalent to 'background', it basically measures 'ambient background' or elemental concentration at the time of sampling at a particular time (Reimann and Garrett, 2005). Furthermore, baseline level should correspond to a range, not to a single value, as it has the disadvantage of not taking into account natural variability on the scale of the area under investigation (Reimann and Garrett, 2005). Several standard methods have been established and widely applied for the determination of baseline values in water and soils (Marandi and Karro, 2008; Reimann et al., 2018; Ander et al. 2013; Rodrigues et al., 2013; Nakić et al. 2007, 2010, Gałuszka, 2007; Reimann and Garrett, 2005; Matschullat et al., 2000; Salomão et al., 2018).

Although regional and national geochemical baseline surveys have been conducted on soils and sediments, the information for local baseline concentrations in surface waters are not available for many countries; this is generally true for Brazil, in particular for the Amazon region. The Itacaiúnas River Basin (IRB), located in the Carajás Mineral Province, is an important river basin in the Brazilian Amazon and contains world-class Fe and Cu mines, as well as Mn, and Ni ones. The rapid increase in the economic activities include: urbanization, and construction of roads and railways; large government projects for rural settlement; and the expansion of cattle farming. This activity has resulted in intense clearing of tropical forest, which has been replaced with pastureland and buildings/roads, which affect the hydrology of the watershed (Souza-Filho et al., 2016). These changes raise a serious environmental concern about IRB's water quality, on which there is little information. A previous geochemical study of surface water samples in the Parauapebas area of the IRB (Ruivo and Sales, 1989) has historical interest, but it does not reflect the present anthropogenic pressures in the basin, and it is limited by the method of sampling and the analytical methods adopted. This work provides a comprehensive look at the hydrogeochemical characterization of the IRB.

Starting in 2016 and continuing today, the Instituto Tecnológico Vale (ITV) is conducting a systematic high resolution geochemical background survey of surficial water, soil and sediments in the Itacaiúnas River Basin under the ItaGMBP using a computer-based framework developed specifically to support this activity. In this project, it was reported the geochemical characterization of surficial water of the sub-basins of the Vermelho and Sororó rivers (Salomão et al., 2018), that provides information about the eastern domain of the IRB. The present study covers the entire basin (approximately 41,500 km^2) from which 1429 samples (including 55 duplicates) from ≈900 sites at a density of 1 sample per micro-basin were collected during both

dry and rainy periods. The high-density survey concentrated on the occurrence and distribution of selected metals with the goal of delineating natural and anthropogenic sourcing and to better understand how this type of data can inform a better understanding of surface water risk assessment as compared to typical national and international guidelines.

2. **Study Area**

2.1. Study area

The IRB (05°10´ to 07°15´S latitude, 48°37´to 51°25´ longitude) is located in the Brazilian Amazonia, Carajás region, Pará State, Northern Brazil (Fig. 1, modified from Souza-Filho et al., 2016). The population of the IRB is approx. 700,000 persons in an area of approx. 41,500 km²; the basin is economically important and is intensely mined (Fig. 1). The main tributaries of Itacaiúnas River are the Cateté, Aquiri, Cinzento, Salobo, Tapirapé, and Preto rivers (western side) and Parauapebas, Vermelho, and Sororó rivers (eastern side). The altitude of this region varies from 350 to 900 m in the Serra dos Carajás to 80 to 300 m in adjacent areas. Originally, tropical rainforest was the predominating land cover in the IRB with subordinate mountain savanna, but, at present the tropical rainforest is mostly limited to environmental protected areas and indigenous lands, which cover 11,700 km^2, or approximately a quarter of the total area (Fig. 1); pasture lands are largely dominant while residual, pristine montane savanna over ferruginous canga and urban areas are less common (see Fig. 1).

The climate of IRB is tropical monsoon (Alvares et al., 2013), with annual precipitation of 1899 mm (climatological normal 1981-2010), which mainly occurs during the rainy season from November to May; the dry season extends from June to October (Moraes et al., 2005). The annual evapotranspiration is 1085 mm/year (Silva Junior et al., 2017) and the average streamflow of the Itacaiúnas river at its confluence with the Tocantins river is about 902 m^3/s (1998-2007 period; Pontes et al., 2019). The intense deforestation process suffered by IRB after 1973 caused an increase of temperature (+1.7°C) and the reduction of air relative humidity (-10%) in the basin (Souza-Filho et al., 2016). Besides, Cavalcante et al. (2019) showed an increase of streamflow from 401 mm/year (1973-1984) to 514 mm/year (2005-2016), and emphasized that without an opposite effect of climate variability, the increase of average streamflow in the IRB would be higher.

2.2. Geological setting

The geology of the IRB is very diverse and covers parts of the Carajás Province, the Bacajá Domain of the Transamazonian Province, and the Araguaia Belt (Fig. 2, Vasquez et al., 2008, modified). The Carajás Province was formed in the Archean and includes the Carajás Basin in the center and the Canaã Carajás, Sapucaia, and Rio Maria domains in the south of the IRB

(Fig. 2, cf. Dall'Agnol et al., 2017). The Bacajá Domain occupies the northern portion of the IRB and consists of Neoarchean and Paleoproterozoic units. Finally, the Araguaia Belt is situated in the eastern portion of the basin and is comparatively younger, having formed at the end of the Neoproterozoic and beginning of the Phanerozoic. For the purpose of geochemical mapping, the basin can be subdivided into four large units described in the following (Fig. 2b, c):

Canaã dos Carajás, Sapucaia, and Rio Maria domains: this segment of the basin has Mesoarchean age (Feio et al., 2013; Moreto et al., 2015) and is formed mainly by granitoid rocks (tonalite-trondhjemite series, calc-alkaline granites, Mg-rich granitoids, leucogranodiorites to leucogranites), associated with orthogranulitic units, and metamafic sequences (greenstone belts). In the Neoarchean, several A-type granites, charnockitic bodies and mafic-ultramafic stratified complexes were formed and they cross-cut the Mesoarchean units (Vasquez et al., 2008; Barros et al., 2009; Feio et al., 2013; Dall'Agnol et al., 2017; Mansur and Ferreira Filho, 2017). This segment of the basin contains the Onça-Puma (Ni) and Sossego (Cu) mines.

Carajás Basin: the Carajás Basin was formed in the Neoarchean (Gibbs et al., 1986; Machado et al., 1991; Martins et al., 2017)and it is dominated by mafic to intermediate metavolcanic sequences and banded-iron formations, which are the primary source of the large Fe deposits of Carajás. These units are cut by Neoarchean granites (Barros et al., 2009; Sardinha et al., 2006). The N4-N5, S11D and Serra Leste iron mines, the Azul manganese mine and the Salobo copper mine are located in this segment. Paleoproterozoic, anorogenic, A-type granites are widespread in the Carajás Province (Dall'Agnol et al., 2005; Teixeira et al., 2017) and are intrusive in the Archaean units (Fig. 2c).

Bacajá Domain: the most widely distributed unit in the IRB that covers the Bacajá Domain (Fig. 2b, c) is formed by reworked high-grade charnockite rocks with subordinate mafic ortogranulite and metasedimentary granulites (Vasquez et al., 2008). Some supracrustal units, including the metamafic Tapirapé rocks, and the metassedimentary Buritirama lithotypes, are also found in this domain. This portion of the basin contains the Buritirama manganese mine. Araguaia Belt: The main units of this tectonic domain within the IRB are composed of anchimetamorphic to low-grade metamorphic rocks (Fig. 2c). Besides these, mafic-ultramafic complexes with associated deep-sea sediments also occur (Vasquez et al., 2008).

3. Materials and Methods

3.1. Strategies and computer-based framework for high density sampling

A total of 1429 (including 55 duplicates) samples were collected in the rainy (February to June, 720 samples) and dry season (July to November, 638 samples), of 2017, with a sampling

density of one stream water sample per microbasin of the IRB. The microbasins were identified using remote sensing techniques. The field and laboratory work received support for sample collection, data storage, screening, and validation from a computer-based framework which was developed in the ItacGMBP of ITV. The framework is composed of three main components: (i) an iPad application for sample collection developed in Swift; (ii) a server back-end written in Java which receives data from the iPads in the field, and acts as a central repository for sample data sharing and synchronization between different field teams; and (iii) data validation and reporting scripts developed in R (R Core Team, 2018). Data screening and validation is active within all three components. The iPad application ensures samples are collected from the correct locations, validates sample data input, and prevents field teams from collecting multiple samples in the same micro-basin (except for duplicates). The server back-end performs additional validations to ensure uniqueness of samples. Finally, R scripts generate reports and statistical plots, match data from the laboratory with their corresponding samples in the database and detect anomalous results due to laboratory error. In short, the computer-based framework provides fast data processing and early error detection which enable the high-density survey presented in this work.

Sample collection avoided roads, and any disturbed areas, in the third order stream, in the middle of the water flow, in a location upstream from the collection point of the stream sediments, to be representative of the microbasin. Representative water sample were taken from second order stream in areas of poor accessibility. A limited number of microbasins could not be sampled, these included the microbasins located on the Xikrin-Cateté indigenous Land and those of two indigenous lands in the Sororó Sub-basin (Fig. 1). During the dry season, this number increased significantly because of the intermittent character of part of the local drainage, particularly in parts of the Sororó, Vermelho, and Parauapebas sub-basins. Duplicate samples were collected immediately after the first samples; one duplicate was collected for each 20 samples.

The sampling and preservation of water samples and analytical methods used for the determination of the variables obeyed the procedure and methodologies recommended in the Standard Methods for the Examination of Water and Wastewater (SMWW, methods 1060 and POP LB 010; APHA 2012). The physico-chemical parameters such as pH, EC, dissolved oxygen (DO), temperature, and redox potential (Eh) were measured in situ at each point with a multi-parameter probe (HI 98194 from Hanna Instruments®) and two separated samples were then collected. A first sample was stored in a 30 ml high density polyethylene bottle (anions determination / non-purgeable organic carbon - NPOC), and a second one in a 60 ml high density polyethylene bottle (metal element analysis). All samples were refrigerated after

collection until dispatched for analysis. The unfiltered water samples used to determine metals were acidified with 1M ultra-pure nitric acid (pH < 2) at the time of collection.

3.2. Chemical analysis and Quality control

Water samples were submitted to the certified laboratory of Bioagri Ambiental Ltda, Brazil, for chemical analysis. The total content of twenty-three elements (Ag, Al, As, Ba, Be, Ca, Cd, Co, Cr, Cu, Fe, Hg, K, Mg, Mn, Mo, N, Na, Ni, Pb, Se, V, and Zn) were analyzed by inductively coupled plasma mass spectrometry (ICP-MS). Anions (F^-, Cl^-, NO_3^-, and SO_4^{2-}). For total phospohrous (TP), samples were digested using sulfuric acid at pH <2 and then analyzed colorimetrically. A summary of the analytical results and detection limits (DL) of these elements is shown in Table 1. The reliability of the data was evaluated by determining the Relative Percentage Differences (RPD) from field duplicate samples (N=55) and more detailed information is provided in the Supplementary material (Fig. 1SM). The overall RPD of the dataset is ±15% for the physico-chemical parameters and most of the metals, which implies that the overall behavior of chemical parameters displays an acceptable variation and demonstrates a high level of analytic precision. There was poor reproducibility (> ±30%) in the case of TP, NO_3, and B; this is probably due to their very low concentrations. Elements with > 70% of samples with contents below the DL were not used for multivariate statistical analysis.

3.3. Hydrogeochemical maps

The World Geodetic System 1984 (WGS84) was used to construct spatial geochemical maps prior to applying the baseline survey methods used in this study. The catchments basins were delimitated via algorithm-based, QGIS software (Quantum GIS Development Team 2009), using a digital elevation model (DEM) from Shuttle Radar Topography Mission (SRTM) conducted by the United States Geological Survey (USGS) (freely available online at https://earthexplorer.usgs.gov/). The contouring and coloring on the maps to show the distribution of elements were defined considering the analytical results for above detection limits data for each element. The resulting intervals on both rainy and dry seasons are comparable; the maps were visualized using ArcGIS 9.3 software.

3.4. Data processing and statistical methods

Descriptive statistics for each parameter were computed on both un-transformed and log10-transformed data after verifying anomalous results due to laboratory error or contamination. Samples below the limit of detection (LD) were assigned a value 1/2 LD before the analysis. Exploratory data analysis (EDA; histograms, density trace, boxplots, and QQ plots) was employed to determine the overall data distribution, multi-modality, and to define outliers in the dataset (Reimann et al., 2005). Correlation analysis using the Spearman rank method in log-

transformed data after excluding the parameters that contained significant numbers of results below DL was used to identify relationships between environmental variables.

Elemental concentrations were used to calculate baseline survey levels; several methods can be used to calculate this as long as the method considers the statistical properties of the geochemical background (Reimann et al., 2005). Typical parametric statistical calculations, that require a normal distribution of the data (Reimann and Filzmoser, 2000), were not used due to the multimodal nature of the data and the occurrence of outliers (Reimann and Filzmoser, 2000). Therefore, estimation of baseline levels was carried out using robust statistical techniques such as ´M_{MAD}´, the median ± 2 Median Absolute Deviation (MAD), Tukey´s inner fence 'TIF', using the upper whisker of a Tukey's box plot as calculated by the 3rd quartile + 1.5IQR (interquartile range) and percentile-based approach with 75^{th}, 90^{th}, 95^{th}, and 98^{th} percentile of a given log-transformed dataset (Ander et al., 2013; Reimann et al., 2018; Reimann and de Caritat, 2017). Cumulative frequency distribution (CFD) curves were also plotted on log-transformed data to determine the upper turning points that separate two datasets (Matschullat et al., 2000). Furthermore, iterative 2σ-technique (I-2σ) and Distribution Function (DF) were used based on the assumption that all values beyond the mean ± 2σ and median, respectively are omitted from the dataset and the new mean ± 2σ range is calculated using the reduced data (Matschullat et al., 2000; Urresti-Estala et al., 2013). All the baseline calculations were undertaken using R (R Core Team, 2018), SPSS, and the VB Background® freeware (Nakić et al., 2007).

4. Results

4.1. Surface water characteristics and seasonal variation

Data for 36 parameters including minimum, mean, 50th percentile (median), maximum, standard deviation (SD), and coefficient of variation (CV), along with detection limit (DL) and proportion of samples <DL, in both dry and rainy periods are presented in Table 1; the quartile distribution of selected parameters are shown in Fig. 3a. A complete table for all elemental data can be found in the Supplementary Material (Table 1SM). Median values are statistically a more robust measure of central tendency than means and can be used for comparison purposes along with their quartile distribution (Reimann et al., 2005). According to the combined results in Table 1 and Fig. 3a, the concentrations of several parameters, such as turbidity, TP, Fe, Al, Mn, Cr, V, and Ni are significantly different in the dry and rainy periods. The coefficient of variation (CV%) reflects the degree of variability with respect to the metal concentrations (CV ≤ 20%, low; 21% ≤ CV ≤ 50%, moderate; 51% ≤ CV ≤ 100% high; CV > 100%, is exceptionally high variability) (Tume et al., 2018). Except for pH and temperature, the degree of variability for most of the parameters is high to exceptionally high, which indicates that multiple factors or

processes are contributing to the variability. The temperature does not vary considerably between the rainy and dry period with median values of 25.8 ^{o}C and 25.48 ^{o}C, respectively. The water in the basin is neutral to slightly alkaline, with median pH of 6.96 and 7.17, respectively, in the rainy and dry period. Although the maximum EC occurs in the dry period, the mean and median values were higher during the rainy period (90 µS/cm^{-1}, and 71 µS/cm^{-1}, respectively). Similarly, TDS is higher in the rainy period (median of 71 mg/L) than in the dry period (median of 66.5 mg/L). The higher EC and TDS in the rainy period may be due to more intense catchment erosion and run-off that leads to an increase in dissolved ions. Turbidity shows exceptionally high variability in the basin and significantly higher values in the rainy period (0.05 – 930 NUT, median of 21.2) than in the dry period (0.05 – 557 NTU, median of 13.9).

The concentrations of all major cations in the waters of the IRB show significant variability but were significantly lower when compared to the values reported for global river water quality (Meybeck and Helmer, 1989). The highest maximum median concentration of Na occurs in the rainy period, followed by Ca>Mg>K, while in the dry period the order is K>Ca>Mg> Na. Median values for Ca and Na are also higher in the rainy season than in the dry season, the converse is true for K and Mg. The anion chemistry shows that HCO_3 is dominant in waters, followed by Cl, F, NO_3 and SO_4. On average, HCO_3 accounts for 80% of the total anions in the surface water and most of the water samples are characterized as Ca-HCO_3 and mixed Ca-Na-HCO_3 types (Fig. 4a). Fig. 4b shows the relationship between TDS and weight ratio of Na/(Na+Ca) and the main processes controlling water composition: data plotting in the middle part of the diagram are indicative of rock weathering as the dominant factor controlling major ion chemistry, except for a few samples which could be influenced by increased precipitation.

Pristine waters contain virtually every element of the periodic table. Anthropogenic forcing leads to perturbations in natural elemental assemblages, usually resulting in higher concentrations, with concomitant impact on aquatic environments. In this study, 30 metals were analyzed, out of them 7 elements (W, Cd, Mo, Ag, Ce, La, and Tl) were totally not detected, so these elements were not discussed in this study. Of the detected elements, only Mn was higher in the dry period, while Fe, Al, Cr, V, Zn and other elements, were higher in the rainy period (Table 1). Compared with CONAMA 357/05 resolution for class 2 waters, except Mn, most elements occur within the recommended guidelines.

4.2. Statistical analysis

An assessment of data distribution was made prior to further statistical analysis. Except DO, pH, and temperature, the mean values of untransformed data of most of the parameters are higher than the median value, indicating far from normal distribution (Table 1). To stabilize the variances, logarithmic (log10) transformation of these data was performed (cf. Table 1 and Fig.

2SM). As shown in Fig. 2SM, the distribution of original (raw) data is asymmetric and right-skewed, with longer tails at higher concentrations due to the presence of a relatively small number of high values. Transformation substantially improves distribution, resulting in an almost symmetric distribution, but not all distributions conformed to normality even after log transformation, which supports the fact that a normal distribution is not typical of geochemical data as the natural occurrences of elements are significantly affected by multiple sources (Reimann and Filzmoser, 2000). Therefore, statistical methods that are least influenced by data distribution (i.e. non-parametric methods) were used. Furthermore, logarithmic transformation is more robust against the effect of data outliers, which is common in geochemical datasets, giving more weight to the use on log-transformed data.

Spearman rank correlation coefficients are given in Fig. 3b; except for correlations marked as '×', the remaining values are significant at p-values ≤0.0001. This shows that the major ions Ca, Mg, Na, HCO_3, along with EC and TDS in both rainy and dry periods were highly correlated with each other ($p \leq 0.0001$), indicating they are involved in similar rock weathering reactions. Turbidity shows high positive correlation with Fe, Al, and TP in the dry period and with Al in the rainy period. Fe and Mn are significantly correlated with each other in both periods. Cr is positively correlated with Ni in both periods. Cu shows positive correlation with SO_4 in both periods. V shows positive correlation with Cr and Ti in both periods, and additionally with Al in the rainy period.

4.3. Spatial distribution – geochemical maps

Fig. 5 shows the spatial distribution for Fe, Mn, Al, Ni, Cu, and Ba in the rainy and dry periods. Higher concentrations occurred mostly in the rainy period. Fe and Al show similar patterns, and are mainly concentrated in the Sororó, Vermelho (Araguaia belt area), and upper Parauapebas sub-basins, and in the northwestern portion of the Itacaiúnas basin, in the Bacaja domain. The behavior of Mn during the rainy season is similar to those of Fe and Al, but in the dry season it is relatively more abundant and differs from the other elements. Although Cu and Ni concentrations are very low, the maps show contrasts in regional distribution. Cu is enriched towards the center of the basin along two approximately east-west zones that follow the north and south copper belts (Moreto et al., 2015) while Ni and is enriched near the occurrences of mafic-ultramafic complexes (Onça-Puma, Vermelho and Luanga). Ba has a broadly similar behavior during both periods but its distribution is clearly different than the other metals. Ba is mainly concentrated in the northern and southern portions of the basin and display lower occurrence in the Carajás basin, and lowest in the Araguaia belt (Fig. 5). The distribution maps of SO_4 and NO_3 are provided in the supplementary material (Fig. 3SM).

4.4. Baseline threshold values

Table 2 shows the B_{TVs} of 17 elements in both dry and rainy periods calculated by using different methods such as median + 2MAD, TIF, iterative-2σ, distribution function, percentiles (75^{th}, 95^{th}, 98^{th}) and CF diagram, along with CONAMA class 2 water quality limit when available. The estimation of baseline values is strongly dependent on the number of results that are <DL. Estimation of baseline levels for As, Se, and Pb were strongly limited for most of the methods due to very high percentages (84 to 99%) of results <DL. In general, for elements having values where the results of more than 50% of the samples are <DL statistical methods such as iterative-2σ, distribution function and median + 2MAD are strongly limited. This is the case for Cu, Ni, Cr, V, Co, and Sn during the rainy season. In the case of the TIF method, its application is limited only when more than 77% of the results are <DL so that it was useful for this work.

The B_{TVs} were highly variable between the dry and rainy periods and also varied significantly between methods (Table 2). The estimated 'natural' B_{TVs} (NB_{TVs}) and 'ambient' B_{TVs} (AB_{TVs}) are marked in **bold** and ***Italic***, respectively in Table 2 (see "Discussion" for the use of methods for this estimation) and shown in Fig. 6 for selective elements.

5. Discussion

5.1. Chemistry and quality of surface waters

The Itacaiúnas river surface waters are predominately characterized by near-neutral to slightly alkaline pH with very high concentrations of Fe and Mn. The correlation between pH and Fe plus Mn is poor, suggesting that low pH is not required to explain Fe and Mn loading in these waters. The levels of bicarbonate in water directly influence the pH. The poor relation between pH and SO_4^{2-} indicates that some low pH values may not have originated through sulfide oxidation. As was pointed out by Medeiros et al. (2017), in other parts of the Amazon basin, this may be due to organic decomposition and leaching of fulvic and humic acids mitigated by microbiological activities in soils and riparian zones, under natural condition. This is supported by the simultaneous decrease of pH and DO during the rainy period, which suggests that significant amounts of organic matter were being released into the rivers, creating a high oxygen demand. The high turbidity levels during the rainy period are due to increased surface runoff that increases the transport of suspended particles, such as silts, planktons, clays, organic matter and other microscopic or decomposed organisms. Moreover, the positive correlation between Al and turbidity indicates that high Al could be associated with suspended particles such as colloidal Al derived from kaolin and Al-rich soils of the region. TDS and EC are higher during the rainy period in the southeastern part of the basin and are probably related to more intense leaching from multiple sources, and are mainly controlled by the erosion of the

weathered surficial materials, which is strongly accelerated in deforested areas (Levy et al., 2018; Nóbrega. et al., 2018).

A Gibbs Plot (Fig. 4b) of TDS vs Na/(Na+Ca), describing 3 main fields (evaporation-crystallization; rock weathering; precipitation) was used to explain the processes controlling the hydrogeochemistry of the IRB (Chakrapani, 2005). As shown, rock/mineral weathering, followed by precipitation to a lesser extent, were the main processes controlling surface water chemistry. Ca-HCO_3 and Ca-Na-HCO_3 define the major water types in the basin (Fig. 4a), showing the mixing of alkali and alkaline-earth elements and dominance of weak acidic anions over strong acidic anions (i.e., HCO_3 > Cl+SO_4). This supports the importance of carbonic acid weathering, inducing dissolution of primary silicate minerals such as alkali-feldspars, plagioclases, pyroxenes, etc. (Tamez-Meléndez et al., 2016). The stoichiometric relationship between dissolved ions are used to unravel the origin of solutes. In general, the molar ratios of Mg/Na and Ca/Na close to 1:1 are indicative of silicate weathering, while higher ratios, close to 100:100, implies carbonate weathering, as reported in literatures (e.g., Gurumurthy et al., 2012, and references therein). In the studied waters, these values are close to 1:1 demonstrating that silicate weathering is the major contributor to the ionic chemistry. In addition, there is a strong positive correlation among Ca, Mg, Na, and K further substantiating a common source for major cations, mainly feldspars and mafic minerals contained in the underlying silicate rocks. This interpretation is consistent with the regional geological setting (Fig. 2). Carbonic acid facilitates the breakdown of silicate minerals. The reactions involved in this process are accompanied by the release of base cations and cause an increase in HCO_3 in the water. Although, the SO_4^{2-} concentration is very low, its positive correlation with Cu indicates that its distribution is geologically controlled (Fig. 3SM), mainly by sulfide minerals, abundant in copper mineralized zones of the basin.

Cl^- in water can originate from various sources including atmospheric deposition as well as from the catchment rocks. The relationship between Na and Cl is frequently used to determine the source of Cl in natural water. When halite dissolution is predominant, it typically results in a molar ratio of 1:1 of Na/Cl, whereas a molar ratio >1 indicates an origin from silicate weathering (Meybeck, 1987). The molar ratio of Na/Cl in the study area is > 2, suggesting that Cl is mostly from the weathering of silicates rather than from halite (Ghrefat et al., 2013). This hypothesis is favored by the high Cl content of micas and amphiboles of some Archean granites and also of the country rocks of copper ore in the Sossego mine (Dall'Agnol et al., 2017; and references therein). In general, F- is usually derived from the weathering of fluoride bearing, rock-forming minerals like muscovite, biotite, fluorite, fluoro-apatite etc. The observed low concentrations of fluorine in water can be due to the low F content in the Archean rocks that are

largely dominant in the catchment of the study area (cf. Dall'Agnol et al., 2017), compared to the F-rich Paleoproterozoic anorogenic granites (Dall'Agnol et al., 2005).

5.2. Metal Sources in relationship to geological setting and land use change

The occurrence and spatial distribution of trace metals reflect different local geological and anthropogenic factors active in the basin. The Itacaiúnas basin shows strong geological contrasts between the four distinct tectonic domains (Fig. 2). This contributes to significant variability in the natural occurrence of major and trace elements. Concentrations of Fe and Mn are high when compared to the CONAMA 357/05 and WHO limits. The Serra Leste, N4-N5, and S11D iron mines, and several other iron deposits in the central area of the IRB, occur mainly in the Carajás basin (Fig. 2), but spatial distribution maps show that the influence of Fe mines and of iron-rich rocks like banded-iron formations do not seem relevant (Fig. 5). The same is true for Mn distribution relative to the Azul and possibly the Buritirama manganese mines (Fig. 1). In fact, Fe, as well Mn and Al, shows notably higher concentrations in the Vermelho, Sororó, and upper Parauapebas sub-basins in the eastern and southern areas of the Itacaiúnas basin (Fig. 5). Relatively high Fe in surficial waters were also observed around the N3 and N4WSul areas, which are considered pristine areas (Teixeira, 2016). These areas are situated in the Carajás National Forest, a protected area in the vicinity of N4 and N5 Fe deposits of northern Serra dos Carajás (Fig. 1). However, in this case the Fe concentrations in the water are lower than in areas external to the Carajás mosaic, that assembles protected areas with preserved pristine tropical forest; this further substantiates that the Fe enrichment in surficial water of some areas of the basin is not due to Fe mining activities. Furthermore, it is interesting to notice that the Fe concentrations increase in areas highly impacted by local anthropogenic activities, mainly land use change. Souza-Filho et al. (2016) demonstrated that the main land use change in the basin was conversion of tropical forest to pasture. This is commonly seen in the Amazon region and significantly affects the local hydrological conditions (Levy et al., 2018; Nóbrega et al., 2018). Hence, higher concentrations could be favored by deforestation that leads to high runoff and erosion of exposed soils and catchment rocks including ferruginous and aluminous crusts. This is consistent with the observation of higher occurrence of most elements in water during the rainy period as noted by Salomão et al. (2018) in the sub-basins of Vermelho and Sororó rivers of the IRB.

Similar distribution and positive correlation between Fe and Mn indicate a similar source for both elements. However, Mn differs from Fe because it is enriched during the dry period, unlike Fe. This could be due to a biogeochemical control which facilitates reduction of Fe^{3+} and Mn^{4+} associated with organic matter, caused by the diminution of available oxygen, which is also supported by the strong negative correlation between Mn and DO. Because the kinetics of Mn oxidation are considerably slower than those for Fe, the precipitation of Mn

takes a longer time than precipitation of Fe, thus, Mn concentration increased over Fe (Stumm and Morgan, 1996). Furthermore, it is generally known that when Mn is reduced it is not removed from water in the presence of ferrous iron at concentration >1 mg/L (Younger et al., 2002). This can explain the cause of high Mn in the dry period.

The behavior of Cu, Ni, Cr, and Ba is entirely distinct from Fe, Mn, and Al, and there is strong evidence that it is controlled by geology. In the case of copper, anomalously high values are related to the large copper mineralized zones (northern and southern copper belts), where mines and deposits of copper are concentrated. Positive correlation between SO_4 and Cu is attributed to the dominance of sulfide mineralization in the area. The Ni and Cr distribution, on the other hand, seems to be controlled by the occurrences of Archean or Neoproterozoic mafic-ultramafic stratified complexes. Finally, higher values for Ba are noted in the areas dominated by granitoid or granulitic rocks that contain Ba-enriched feldspars and biotite. These rocks are located in the Canaã dos Carajás, Sapucaia and Rio Maria domains in the south and in the Bacajá domain in the north.

Overall, the fact that higher concentrations of most of the metals occur in the rainy season indicates that hydrological conditions exerted strong influence in the metal load in water by more intense leaching of exposed soils and weathered minerals/rocks. Except locally, there is no evidence that anthropogenic activities have further increased metal concentration over natural processes.

5.3. Anthropogenic influences

Except for mining, industrial activity is scarce in the IRB. Siderurgical plants producing mostly pig iron and iron alloys are concentrated near Marabá. Mining is mainly limited to extraction, and copper ore is submitted to treatment to concentrate copper near the Salobo and Sossego mines and there is also a metallurgic plant for producing Ni alloys near the Onça-Puma mining district (Fig.1). Some cattle packing plants are also scattered throughout the basin. Agriculture is poorly developed and is generally restricted to small scale familial production. Efforts to install soya beam plantations in the northwestern area of the basin were identified but they are recent and occupy a relatively small area. Apart from mining, the main economic activity is by far cattle production that is largely scattered in the basin, and absent in the environmentally protected areas (Fig. 1). NO_3^- is a major anthropogenic contaminant in surface water and can be used as an indicator of anthropogenic impact. It was not detected in 85% to 89% of the water samples (Table 1), and when present, the average was much lower than the upper limit stated by the CONAMA Resolution (10 mg/l; BRASIL, 2005). The only occurrence of NO_3 excess was noted in a very few samples near the protected area of Igarapé Gelado (Fig. 1; Fig. 3SM), around inhabited areas, and are attributed to the oxidation of nitrogenous human

and animal wastes. Additionally, the molar ratio of Cl^-/Na^+ in all samples is < 1.0 indicating that the Cl content in the water is not a result of anthropogenic activities (Wang et al., 2007). Although, Fe and Mn mines are active in this region, high enrichment of Fe and Mn is not directly related to mining, but rather to specific conditions inherent to the Amazonian region, that where reinforced by land use changes, as already discussed above; this is a general tendency in the Amazon region (SEMAS / PA 2012; Salomão et al., 2018). Furthermore, despite the occurrence of Ni and Cu mines and treatment plants in this region, the very low concentrations of these metals in water, much below to the values defined for CONAMA class II water, along with high pH values and very low SO_4 concentrations, clearly indicate that there is no significant impact of mining in the basin.

5.4. Establishment of baseline threshold values for IRB

From a geochemical point of view, the term "geochemical background" was first used by exploration geochemists for prospection purposes (Hawkes, 1976). Currently, this is being used as a reference to quantitatively distinguish between natural and anthropogenic elemental contributions (Reimann and Garrett, 2005; Reimann et al., 2005). The upper limit of background variation is known as threshold limit, above which the samples are considered at being risk and further investigation will be needed to evaluate their environmental conditions. However, determining natural background concentrations in water is a complex task due to the variability of climatic, hydrology, biological, and anthropogenic factors, working in the system (Gałuszka, 2007). Geochemical 'baseline' is sometimes used as equivalent to 'background', but it differs from background because basically it measures elemental concentration at the time of sampling and it is more useful as a single data point, against which future changes can be compared (Reimann and Garrett, 2005). Nevertheless, the term "baseline/background levels" is used in a number of different senses, e.g. "natural baseline" and "ambient baseline", which reflect a different understanding or definition of what is regarded as being "natural" and/or "not natural" (Tidball and Ebens, 1976; Salminen and Gregorauskiene, 2000; Wendland et al., 2008). In this context, the present study focuses on estimating different baseline levels and this is estimated separately for the two distinct periods as the water quality is varied significantly seasonally.

The occurrence and spatial distribution of elements, as well as the descriptive statistics, demonstrate that there is significant variation in metal concentrations between the rainy and dry periods, thus making it necessary to establish separate baseline levels for each. The estimated baseline concentrations clearly show that higher values for most metals occur in the rainy period. When comparing the results obtained with the different statistical methods (Table 2), it is evident that iterative-2σ technique estimates are very conservative, because it results in the lowest values for baselines, close to 75^{th} percentile (Table 2). These conservative/low levels

may be suitable for legislative protection of the environment. Matschullat et al. (2000) explained that iterative-2σ and DF techniques removed significant numbers of outliers and produced promising and realistic results, and thus they can be more appropriate for estimation of pristine/natural geochemical background levels. Because of the omnipresence of human impacts in the case study area and the surface water is exposed to atmospheric conditions, it will be very difficult to define the strictly "natural" baseline levels. Against this baseline a more pragmatically understanding of the term "natural baseline level" needs to be used, which can consider the human impacts on surface water to a certain degree as inevitable (Wendland et al., 2008). Therefore, we define "natural baseline level" as the concentration of a given element which is considered as the least degraded with low or no significant level of anthropogenic influence. The 'iterative 2σ', which is providing a very restrictive or conservative estimates, was assumed as 'natural baseline threshold values, 'NB_{TVc}'. The NB_{TVc} for different elements are given in Table 2. For Cu, in the rainy period, this technique was not appropriate, so the estimated baseline value by DF was used. Furthermore, neither iterative-2σ or DF were able to provide suitable baseline estimates for Ni, Cr, Co, B, V (in the dry period), and Sn (in the rainy season), because of the significant percentage of observations <DL. In these cases, CF was the chosen method for the estimation of their NB_{TVc}. Overall, higher NB_{TVc} values for metals in the rainy period are due to the influence of natural conditions that were discussed above (Fig. 6). However, NB_{TVc} have delineated a high number of sites which need attention or further investigation, which may sometimes be counter-productive and costly, tending to hinder the achievement of a real goal and taking attention from the few sites that may really have problems. In addition, the use of NB_{TV} is better for identifying the influence of natural factors. However, the geochemical baseline should also consider the sum of natural geogenic plus anthropogenic factors, mainly from diffuse sources (Salminen and Gregorauskiene, 2000; Jarva, 2016). This can be applied in Amazonia, particularly in the IRB, where intense deforestation occurs along with land use change and mining activity, i.e., multiple contributing factors. This realistic approach is needed to estimate the natural plus the diffuse source on geochemical baseline concentrations. The resulting values can be called as ambient baseline threshold (AB_{TVs}), following the concept of Ander et al. (2013).

Several other methods can be used to define AB_{TVs} (Table 2). The Median+2MAD values methods which closure at the 90^{th} and 95^{th} percentiles result in a higher number of sites requiring further investigation. Although the TIF is considered one of the best methods to identify the sites that will need closer attention (Reimann and Caritat, 2017), depending on the data distribution, it does not assume the presence of outliers. The percentile-based approach, such as 98^{th} percentile, is widely used and provides a fixed number of cases that are in greater need of attention (Reimann et al., 2018). Furthermore, the 98th percentile method often

coincides with a break in the CP distribution that can correspond to the upper threshold. Thus, the 98th percentile method appears to be most appropriate to define the AB_{TVs} limit (cf. values in Table 2, Fig. 6). The estimated NoBT threshold for most of the elements, except Mn, were higher in the rainy period due to more intense leaching of catchment rocks, and related to the influence of anthropogenic activities, mainly deforestation. The distinct behavior of Mn can be explained by biogeochemical processes and by its different oxidation behavior relative to Fe. For elements such as Pb, As, and Se, which have nearly 90% or greater sample results below DL, the AB_{TVs} was not calculated. For these elements, it was decided that the 95th percentile (Pb) and 98th percentile (Se and As, in the rainy period, and As) should be considered as their baseline limit. Higher AB_{TVs} for most of the metals in the rainy period may be due to more leaching of catchment lithology including the mineralized rocks, so it can also be considered as geogenic/mineragenic baseline. This can be more interesting for the copper belts in Itacaiúnas basin, in order to identify the influence of mineral deposits and associated ore vein on water quality.

5.5. Implication of site-specific baseline studies for environmental studies

Comparison with national/international water quality guidelines is a typical procedure to evaluate the quality of surface water and identify contamination. In Brazil, that evaluation is being carried out following CONAMA Resolution No. 357/2005 (BRASIL, 2005). If the concentrations do not exceed the legal limit, the water quality is adequate and it is potable. However, this can be disputable, as the national guideline values are often simply adopted from other countries or continents, without considering that water quality is highly dependent on local hydrological conditions, geological setting and other local activities such as land use change, urbanization and agricultural activities which may differ strongly from one region to another (Reimann et al., 2018; Arpine and Gayane, 2016). As a result, the local baseline concentrations of metals can be unique for regional background/national guidelines. In this context, the application of improper guidelines, sometimes either over or underestimate the risk, resulting in unnecessary economic and/or ecological cost. Stream waters of the IRB represent a remarkable example of how local factors such as catchment lithology and land use change can control the baseline water conditions, e.g., the high concentrations of Fe and Mn, which exceed the acceptable limit when compared with CONAMA and WHO guidelines. Thus, as evidenced in the present work, without a thorough understanding of the local environment, national or international guideline values cannot be simply used as reference values for water quality assessment in any region; rather a site-specific, in-depth geochemical baseline assessment must also be taken into account for a correct evaluation of water quality.

6. Conclusions

The following conclusions arrived from the high resolution hydrogeochemical survey and hydrogeochemical baseline study on Itacaiunas River Basin (IRB), in the Amazon region:

- The water quality of IRB is varied little between seasonal climatic periods, and most of the parameters (except Fe and Mn) were within the limit when compared with CONAMA and WHO guidelines.
- Neutral to slightly alkaline pH with very high concentrations of Fe and Mn, is the common geochemical signature of surficial water in the Itacaiúnas basin.
- Ca-Na-HCO_3 is the dominant water type in the area and silicate weathering was the major hydrogeochemical process controlling water chemistry.
- Seasonality has a significant influence on the concentration of metals, with a tendency to be higher in the rainy period.
- High resolution survey and geochemical mapping allowed the identification of major factors controlling the variability of metals. The spatial distribution of Fe, Al, and Mn cannot be explained by lithological control. Their occurrence and distribution is more likely related to intensely weathered catchment and increase of run-off due to intense deforestation in the eastern and southern portions of the basin. High baseline values of Mn during the dry period are explained by biological processes favoring reducing conditions, while Cu, Cr, and Ni are more influenced by underlying lithology.
- Iterative 2σ followed by DF techniques are the more suitable for the estimation of the natural baseline threshold values 'NB_{TVc}', which is considered as low or no significant level of anthropogenic influence; while 98th percentile is more realistic to define ambient baseline threshold values 'AB_{TVs}' which include both natural and diffuse anthropogenic sources.
- This study demonstrates that site-specific baseline values are crucially important to address the specificities of each local and identify contamination for planning water management.
- The present study estimated the baseline values for the entire basin. More detailed and focused studies should be done in the future for strengthening the effective use of baseline values for environmental risk assessment.

Acknowledgements

This work is part of the Itacaiúnas Geochemical Mapping and Background Project, ItacGMBP, currently being undertaken at Instituto Tecnológico Vale (ITV), Belém, Brazil. This was supported by: Vale (GABAN-DIFN); Conselho Nacional de Desenvolvimento Científico e Tecnológico (CNPq) [DTI scholarship to GNS (Proc. 380.418/2018-5); grants to RD (proc. 306108/2014-3; Proc. 443247/2015-3); and PWSF (306450/2013-5)]. The authors acknowledge two anonymous reviewers for their constructive reviews and to Carlos Augusto de Medeiros

Filho, José Francisco Bêrredo, José Francisco da Fonseca Ramos, Luiz Roberto Guimarães Guilherme, Marcondes L. da Costa and Otavio Augusto Boni Licht, for their scientific collaboration with the Background project.

References

Alvares, C.A., Stape, J.L., Sentelhas, P.C., de Moraes Gonçalves, J.L., Sparovek, G., 2013. Köppen's climate classification map for Brazil. Meteorol. Z. 22, 711–728. https://doi.org/10.1127/0941-2948/2013/0507

Ander, E.L., Johnson, C.C., Cave, M.R., Palumbo-Roe, B., Nathanail, C.P., Lark, R.M., 2013. Methodology for the determination of normal background concentrations of contaminants in English soil. Sci. Total Environ. 454–455, 604–618. https://doi.org/10.1016/j.scitotenv.2013.03.005

Arpine, H., Gayane, S., 2016. Determination of background concentrations of hydrochemical parameters and water quality assessment in the Akhuryan River Basin (Armenia). Phys. Chem. Earth 94, 2–9. https://doi.org/10.1016/j.pce.2016.03.011

Barros, C.E.M., Sardinha, A.S.., Barbosa, J. d. P., Macambira, M.J.B., Barbey, P., Boullier, A.-M., 2009. Structure, petrology, geochemistry and zircon u/pb and pb/pb geochronology of the synkinematic archean (2.7 ga) a-type granites from the carajas metallogenic province, northern brazil. Can. Mineral. 47, 1423–1440. https://doi.org/10.3749/canmin.47.6.1423

Brion, G., Brye, K., Haggard, B., West, C., Brahana, J., 2011. Land-use effects on water quality of a first-order stream in the Ozark Highlands, mid-southern United States. River. Res. Appl 27, 772–790.

BRASIL. Ministério do Meio Ambiente. Resolução CONAMA nº 357, de 17 de março de 2005. Dispõe sobre a classificação dos corpos de água e diretrizes ambientais para o seu enquadramento, bem como estabelece as condições e padrões de lançamento de efluentes, e dá outras providências. Diário Oficial [da] República Federativa do Brasil. Brasília, DF, 18 mar. 2005. Disponível em: <http: http://www.mma.gov.br/port/conama/res/res05/res35705.pdf> Acessed on 15th april 2018.

Caritat, P., Cooper, M., 2016. A continental-scale geochemical atlas for resource exploration and environmental management: the National Geochemical Survey of Australia. Geochemistry Explor. Environ. Anal. 16, 3–13. https://doi.org/10.1144/geochem2014-322.

Cavalcante, R.B.L., Pontes, P.R.M., Souza-Filho, P.W.M., de Souza, E.B., 2019. Opposite Effects of Climate and Land Use Changes on the Annual Water Balance in the Amazon Arc of Deforestation. Water Resouces Research. DOI: 10.1029/2019WR025083.

Chakrapani, G.J., 2005. Major and trace element geochemistry in upper Ganga river in the Himalayas, India. Environ. Geol. 48, 189–201. https://doi.org/10.1007/s00254-005-1287-1

Dall'Agnol, R., Cunha, I.R.V. da, Guimarães, F.V., Oliveira, D.C. de, Teixeira, M.F.B., Feio, G.R.L., Lamarão, C.N., 2017. Mineralogy, geochemistry, and petrology of Neoarchean ferroan to magnesian granites of Carajás Province, Amazonian Craton: The origin of hydrated granites associated with charnockites. Lithos 277, 3–32. https://doi.org/10.1016/j.lithos.2016.09.032

Dall'Agnol, R., Teixeira, N.P., Rämö, O.T., Moura, C.A.V., Macambira, M.J.B., de Oliveira, D.C., 2005. Petrogenesis of the Paleoproterozoic rapakivi A-type granites of the Archean Carajás metallogenic province, Brazil. Lithos 80, 101–129. https://doi.org/10.1016/j.lithos.2004.03.058

Donn., M., Barron., O., Daniel., P., Chris., J., 2010. Surface water quality investigation using high resolution water quality analysers. CSIRO: Water for a Healthy Country National Research Flagship, 72 pp.

Feio, G.R.L., Dall'Agnol, R., Dantas, E.L., Macambira, M.J.B., Santos, J.O.S., Althoff, F.J., Soares, J.E.B., 2013. Archean granitoid magmatism in the Canaã dos Carajás area: Implications for crustal evolution of the Carajás province, Amazonian craton, Brazil. Precambrian Res. 227, 157–185. https://doi.org/10.1016/j.precamres.2012.04.007

Gałuszka, A., 2007. Different approaches in using and understanding the term "Geochemical

background" - Practical implications for environmental studies. Polish J. Environ. Stud. 16, 389–395.

Gałuszka, A., Migaszewski, Z., 2011. Geochemical background - an environmental perspective. Mineralogia 42, 7–17. https://doi.org/10.2478/v10002-011-0002-y

Ghrefat, H.A., Batayneh, A., Zaman, H., Zumlot, T., Elawadi, E., Nazzal, Y., 2013. Major ion chemistry and weathering processes in the Midyan Basin, northwestern Saudi Arabia. Environ. Monit. Assess. 185, 8695–8705. https://doi.org/10.1007/s10661-013-3205-4

Gibbs, A.K., Wirth, K.R., Hirata, W.K., Olszewski, W.J., 1986. Age and composition of the Grão Pará group volcanics, Serra dos Carajás. Rev. Bras. Geociências 16, 201–211.

Gurumurthy, G.P., Balakrishna, K., Riotte, J., Braun, J-J., Audry, S., Shankar, H.N.U., Manjunatha, B.R., 2012. Controls on intense silicate weathering in a tropical river, southwestern India. Chemical Geol. 300-301, 61-69.

Hawkes., H., 1976. The early days of exploration geochemistry. J. Geochemical Explor. 6, 1–11.

Jarva, J., 2016. Geochemical baselines in the assessment of soil contamination in Finland. Geological Survey of Finland, Espoo, pp. 52. http://tupa.gtk.fi/julkaisu/erikoisjulkaisu/ej_096.pdf (accessed 17 December 2018).

Jacobs, S.R., Breuer, L., Butterbach-Bahl, K., Pelster, D.E., Rufino, M.C., 2017. Land use affects total dissolved nitrogen and nitrate concentrations in tropical montane streams in Kenya. Sci. Total Environ. 603–604, 519–532. https://doi.org/10.1016/j.scitotenv.2017.06.100

Johnson, C., Breward, N., Ander, E.L., Ault, L., 2005. G-BASE: baseline geochemical mapping of Great Britain and Northern Ireland. Geochemistry Explor. Environ. Anal. 5, 347–357. https://doi.org/10.1144/1467-7873/05-070

Jorquera, C.O., Oates, C.J., Plant, J.A., Kyser, K., Ihlenfeld, C., Voulvoulis, N., 2015. Regional hydrogeochemical mapping in Central Chile: natural and anthropogenic sources of elements and compounds. Geochemistry Explor. Environ. Anal. 15, 72–96. https://doi.org/10.1144/geochem2013-220

Labuschagne, L.S., Holdsworth, R., Stone, T.P., 1993. Regional stream sediment geochemical survey of South Africa. J. Geochemical Explor. 47, 283–296. https://doi.org/10.1016/0375-6742(93)90071-S

Levy, M., Lopes, A., Cohn, A., Larsen, L., Thompson, S., 2018. Land use change increases streamflow across the arc of deforestation in Brazil. Geophys. Res 45, 1–11.

Lombard, M., De Bruin, D., Elsenbroek, J.H., 1999. High-density regional geochemical mapping of soils and stream sediments in South Africa. J. Geochemical Explor. 66, 145–149. https://doi.org/10.1016/S0375-6742(99)00032-1

Machado, N., Lindenmayer, Z., Krogh, T.E., Lindenmayer, D., 1991. U-Pb geochronology of Archean magmatism and basement reactivation in the Carajás area, Amazon shield, Brazil. Precambrian Res. 49, 329–354. https://doi.org/10.1016/0301-9268(91)90040-H

Mansur, E.T., Ferreira Filho, C.F., 2017. Chromitites from the Luanga Complex, Carajás, Brazil: Stratigraphic distribution and clues to processes leading to post-magmatic alteration. Ore Geol. Rev. 90, 110–130.

Marandi, A., Karro, E., 2008. Natural background levels and threshold values of monitored parameters in the Cambrian-Vendian groundwater body, Estonia. Environ. Geol. 54, 1217–1225. https://doi.org/10.1007/s00254-007-0904-6

Martins, P.L.G., Toledo, C.L.B., Silva, A.M., Chemale Jr, F., Santos, J.O.S., Assis, L.M., 2017. Neoarchean magmatism in the southeastern Amazonian Craton, Brazil: Petrography, geochemistry and tectonic significance of basalts from the Carajás Basin. Precambrian Res. 302, 340–357. https://doi.org/10.1016/j.precamres.2017.10.013

Matschullat, J., Ottenstein, R., Reimann, C., 2000. Geochemical background - Can we calculate it? Environ. Geol. 39, 990–1000. https://doi.org/10.1007/s002549900084

Meybeck., M., 1987. Global chemical weathering of surficial rocks estimated from river dissolved loads. Am. J. Sci. 287, 401–428.

Meybeck, M., Helmer, R., 1989. The quality of rivers: From pristine stage to global pollution.

Palaeogeogr. Palaeoclimatol. Palaeoecol. 75, 283–309. https://doi.org/10.1016/0031-0182(89)90191-0

Monteiro, L.V.S., Xavier, R.P., Hitzman, M.W., Juliani, C., de Souza Filho, C.R., Carvalho, E. de R., 2008. Mineral chemistry of ore and hydrothermal alteration at the Sossego iron oxide–copper–gold deposit, Carajás Mineral Province, Brazil. Ore Geol. Rev. 34, 317–336. https://doi.org/10.1016/j.oregeorev.2008.01.003

Moraes, B.C. de, Costa, J.M.N. da, Costa, A.C.L. da, Costa, M.H., 2005. Variação espacial e temporal da precipitação no Estado do Pará. Acta Amaz. 35, 207–214. https://doi.org/10.1590/S0044-59672005000200010

Moreto, C.P.N., Monteiro., L.V.S, Xavier., R.P, Creaser., R.A., DuFrane, S.A., Melo, G.H.C., Silva, M.A.D., Tassinari, C.C.G., Sato, K., 2015. Timing of multiple hydrothermal events in the iron oxide–copper–gold deposits of the Southern Copper Belt, Carajás Province, Brazil. Miner. Depos. 50, 517–546.

Nakić., Z., Posavec., K., Bačani., A., 2007. A visual basic spreadsheet macro for geochemical background analysis. Ground Water 45, 642–647.

Nakić Z., Posavec K., Parlov J. 2010. Model-based objective methods for the estimation of groundwater geochemical background. AQUAmundi. 1, 65–72.

Nóbrega., R., Lamparter., G., Hughes., H., Guzha., A., Amorim., R., Gerold., G., 2018. A multi-approach and multi-scale study on water quantity and quality changes in the Tapajós River basin, Amazon. Proc. Int. Assoc. Hydrol. Sci 377, 3–7.

Pinto, M., Silva, E., Silva, M., Melo-Gonçalves, P., Candeias, C., 2014. Environmental Risk Assessment Based on High-Resolution Spatial Maps of Potentially Toxic Elements Sampled on Stream Sediments of Santiago, Cape Verde. Geosciences 4, 297–315. https://doi.org/10.3390/geosciences4040297.

Pontes, P.R.M., Cavalcante, R.B.L., Sahoo, P.K., Silva Junior, R.O., Silva, M.S., Dall'Agnol, R., Siqueira, J.O. (2019) The role of protected and deforested areas in the hydrological processes of Itacaiúnas River Basin, eastern Amazonia. Journal of Environmental Management, 25, 489-499.

Plant, J.A., Klaver, G., Locutura, J., Salminen, R., Vrana, K., Fordyce, F.M., 1997. The forum of European geological surveys geochemistry task group inventory 1994-1996. J. Geochemical Explor. 59, 123–146. https://doi.org/10.1016/S0375-6742(97)00008-3

R Core Team, 2018. R: A Language and Environment for Statistical Computing. R Foundation for Statistical Computing, Vienna. https://www.R-project.org.

Reimann., C., Filzmoser., P., 2000. Normal and lognormal data distribution in geochemistry: death of a myth. Consequences for the statistical treatment of geochemical and environmental data. Env. Geol 39, 1001–1014.

Reimann, C., de Caritat, P., 2017. Establishing geochemical background variation and threshold values for 59 elements in Australian surface soil. Sci. Total Environ. 578, 633–648. https://doi.org/10.1016/j.scitotenv.2016.11.010

Reimann, C., Fabian, K., Birke, M., Filzmoser, P., Demetriades, A., Négrel, P., Oorts, K., Matschullat, J., de Caritat, P., Albanese, S., Anderson, M., Baritz, R., Batista, M.J., Bel-Ian, A., Cicchella, D., De Vivo, B., De Vos, W., Dinelli, E., Ďuriš, M., Dusza-Dobek, A., Eggen, O.A., Eklund, M., Ernsten, V., Flight, D.M.A., Forrester, S., Fügedi, U., Gilucis, A., Gosar, M., Gregorauskiene, V., De Groot, W., Gulan, A., Halamić, J., Haslinger, E., Hayoz, P., Hoogewerff, J., Hrvatovic, H., Husnjak, S., Jähne-Klingberg, F., Janik, L., Jordan, G., Kaminari, M., Kirby, J., Klos, V., Kwećko, P., Kuti, L., Ladenberger, A., Lima, A., Locutura, J., Lucivjansky, P., Mann, A., Mackovych, D., McLaughlin, M., Malyuk, B.I., Maquil, R., Meuli, R.G., Mol, G., O'Connor, P., Ottesen, R.T., Pasnieczna, A., Petersell, V., Pfleiderer, S., Poňavič, M., Prazeres, C., Radusinović, S., Rauch, U., Salpeteur, I., Scanlon, R., Schedl, A., Scheib, A., Schoeters, I., Šefčik, P., Sellersjö, E., Slaninka, I., Soriano-Disla, J.M., Šorša, A., Svrkota, R., Stafilov, T., Tarvainen, T., Tendavilov, V., Valera, P., Verougstraete, V., Vidojević, D., Zissimos, A., Zomeni, Z., Sadeghi, M., 2018. GEMAS: Establishing geochemical background and threshold for 53 chemical elements in European agricultural soil. Appl. Geochemistry 88, 302–318. https://doi.org/10.1016/j.apgeochem.2017.01.021

Reimann, C., Filzmoser, P., R.G., G., 2005. Background and threshold: critical comparison of methods of determination. Sci. Total Env. 346, 1–16.

Reimann, C., Garrett, R.G., 2005. Geochemical background—concept and reality. Sci. Total Environ. 350, 12–27. https://doi.org/10.1016/j.scitotenv.2005.01.047

Rencz, A.N., Garrett, R.G., Adcock, S.W., Bonham-Carter, G.F., 2006. Geochemical background in soil and till. Geological Survey of Canada. https://doi.org/Open File 5084

Rodrigues A.S.L., Malafaia G., Costa A.T., Nalini Júnior H.A., 2013. Background values for chemical elements in sediments of the Gualaxo do Norte River Basin, MG, Brazil. Ver. Ciênc. Amb. 7,15-32.

Ruivo, M.L.P., Sales, M.E.C., 1989. Monitoramento da qualidade da água na área do projeto Ferro Carajás- Um subsídio para o estudo ambiental. Bol. Mus. Para. Emilio Goeldi Cienc. da Terra 1, 11–24.

Salminen, R., Tarvainen, T., 1997. The problem of defining geochemical baselines. A case study of selected elements and geological materials in Finland. J. Geochemical Explor. 60, 91–98. https://doi.org/10.1016/S0375-6742(97)00028-9

Salminen, R., Gregorauskiene,V., 2000. Considerations regarding the definition of a geochemical baseline of elements in the surficial materials in areas differing in basic geology. Appl. Geochem. 15, 647-653

Salomão, G.N., Dall'Agnol, R., Sahoo, P.K., Júnior, J.S.F., Silva, M.S., Souza Filho, P.W., Junior, W.R.N., Costa, M.F., 2018. Geochemical distribution and thresholds values determination of heavy metals in stream water in the sub-basins of Vermelho and Sororó rivers, Itacaiúnas River watershed, Eastern Amazon, Brazil. Geochim. Bras. 32, 179 - 197.

Sardinha, A.S., Barros, C.E. de M., Krymsky, R., 2006. Geology, geochemistry, and U–Pb geochronology of the Archean (2.74Ga) Serra do Rabo granite stocks, Carajás Metallogenetic Province, northern Brazil. J. South Am. Earth Sci. 20, 327–339. https://doi.org/10.1016/j.jsames.2005.11.001

Silva Júnior, R.O., Queiroz, J.C.B., Ferreira, D.B.S., Tavares, A.L., Souza-Filho, P.W.M., Guimarães, J.T.F., Rocha, E.J.P., 2017. Estimation of Precipitation and average Flows for the Itacaiúnas River Watershed (IRW) - Eastern Amazonia , Brazil. Revista Brasileira de Geografia Física, 10, 1638-1654.

Simpson, P.R., Breward, N., Flight, D.M.A., Lister, T.R., Cook, J.M., Smith, B., Hall, G.E.M., 1996. High resolution regional hydrogeochemical baseline mapping of stream water of Wales, the Welsh Borders and West Midlands region. Appl. Geochemistry 11, 621–632. https://doi.org/10.1016/S0883-2927(96)00001-7

Simpson, P.R., Edmunds, W.M., Breward, N., Cook, J.M., Flight, D., Hall, G.E.M. & Lister, T.R. 1993. Geochemical mapping of stream water for environmental studies and mineral exploration in the UK. J. Geochemical Explor. 49, 63–88.

Souza-Filho, P.W.M., de Souza, E.B., Silva Júnior, R.O., Nascimento, W.R., Versiani de Mendonça, B.R., Guimarães, J.T.F., Dall'Agnol, R., Siqueira, J.O., 2016. Four decades of land-cover, land-use and hydroclimatology changes in the Itacaiúnas River watershed, southeastern Amazon. J. Environ. Manage. 167, 175–184. https://doi.org/10.1016/j.jenvman.2015.11.039

Tamez-Meléndez, C., Hernández-Antonio, A., Gaona-Zanella, P.C., Ornelas-Soto, N., Mahlknecht, J., 2016. Isotope signatures and hydrochemistry as tools in assessing groundwater occurrence and dynamics in a coastal arid aquifer. Environ. Earth Sci. 75, 830. https://doi.org/10.1007/s12665-016-5617-2

Teixeira., S., 2016. Estudo da qualidade das águas superficiais e estimativa de background na área das minas de ferro da Serra Norte, Carajás. Master Thesis. Instituto Tecnológico Vale. 128p.

Teixeira, M.F.B., Dall'Agnol, R., Santos, J.O.S., de Sousa, L.A.M., Lafon, J.-M., 2017. Geochemistry, geochronology and Nd isotopes of the Gogó da Onça Granite: A new Paleoproterozoic A-type granite of Carajás Province, Brazil. J. South Am. Earth Sci. 80, 47–65. https://doi.org/10.1016/j.jsames.2017.09.017

Tidball, R.R., Ebens, R.J., 1976. Regional geochemical baselines in soils of the Powder River Basin, MontanaWyoming. In: Laudon, R. B. (ed.) Geology and energy resources of the

Powder River Basin. Wyoming Geological Association, 28th Annual Field Conference Guidebook, pp. 299−310.

Tume, P., González, E., King, R.W., Monsalve, V., Roca, N., Bech, J., 2018. Spatial distribution of potentially harmful elements in urban soils, city of Talcahuano, Chile. J. Geochemical Explor. 184, 333–344. https://doi.org/10.1016/j.gexplo.2016.12.007

Urresti-Estala, B., Carrasco-Cantos, F., Vadillo-Pérez, I., Jiménez-Gavilán, P., 2013. Determination of background levels on water quality of groundwater bodies: A methodological proposal applied to a Mediterranean River basin (Guadalhorce River, Málaga, southern Spain). J. Environ. Manage. 117, 121–130. https://doi.org/10.1016/j.jenvman.2012.11.042

Vasquez, L.V., Rosa-Costa, L.R., Silva, C.G., Ricci, P.F., Barbosa, J.O., Klein, E.L., 2008. Geologia e recursos minerais do estado do Pará: Sistema de Informações Geográficas – SIG: texto explicativo dos mapas geológico e tectônico e de recursos minerais do estado do Pará.

Wang, X., Lu, Y., Han, J., He, G., Wang, T., 2007. Identification of anthropogenic influences on water quality of rivers in Taihu watershed. J. Environ. Sci. 19, 475–481. https://doi.org/10.1016/S1001-0742(07)60080-1

Wendland, F., Berthold, G., Blum, A., Elsass, P., Fritsche, J.G., Kunkel, R., Wolter, R. 2008. Derivation of natural background levels and threshold values for groundwater bodies in the Upper Rhine Valley (France, Switzerland and Germany). Desalination, 226, 160-168.

Younger, P.L., Banwart, S.A., Hedin, R.S., 2002. Mine Water, Environmental Pollution. Springer Netherlands, Dordrecht. https://doi.org/10.1007/978-94-010-0610-1

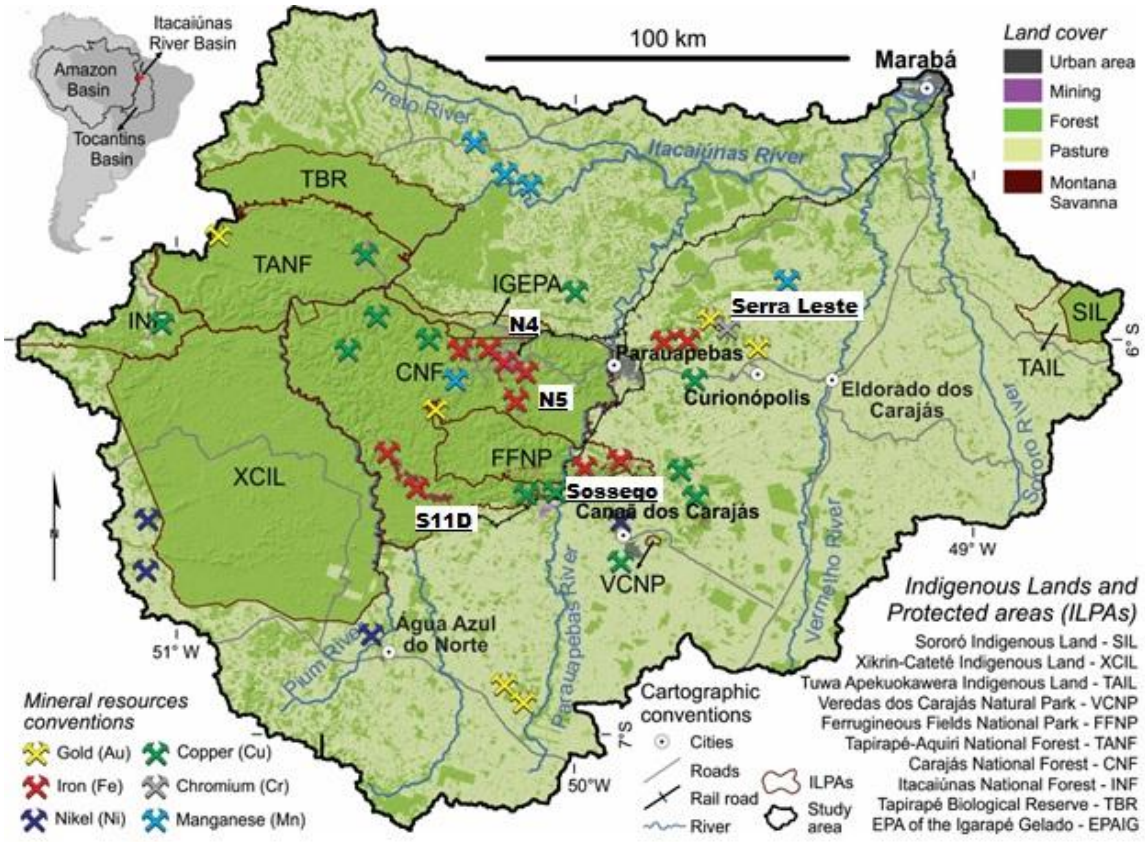

Fig. 1. Map of the Itacaiúnas River Basin located in the Carajás region in the Brazilian Amazonia, Pará state, north of Brazil. The location of main cities and the major land use and land cover, including mines, and mineral deposits, and the indigenous lans and protected areas are indicated in the study area (Modified from Souza-Filho et al. 2016).

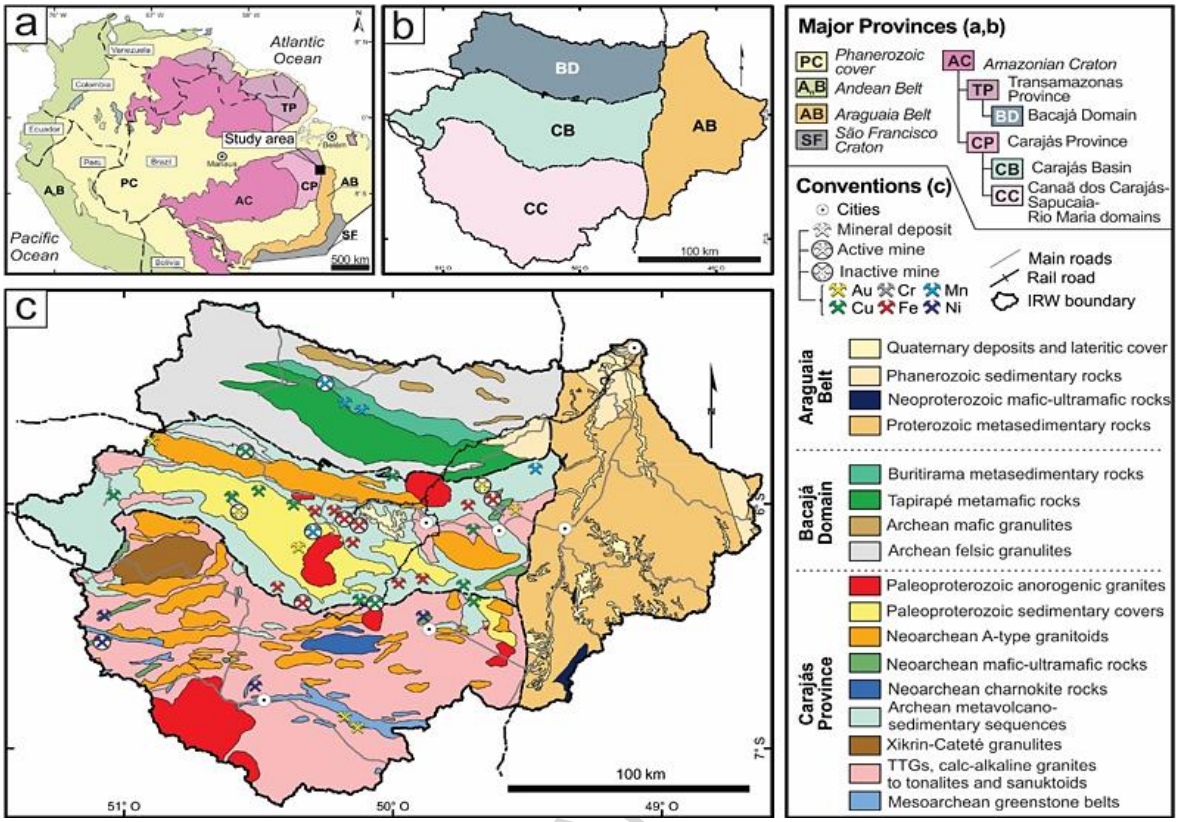

Fig. 2. Simplified geological map of the Itacaiúnas basin (modified from Teixeira et al.,2017; Vasquez et al., 2008; and Alvarenga et al., 2000).

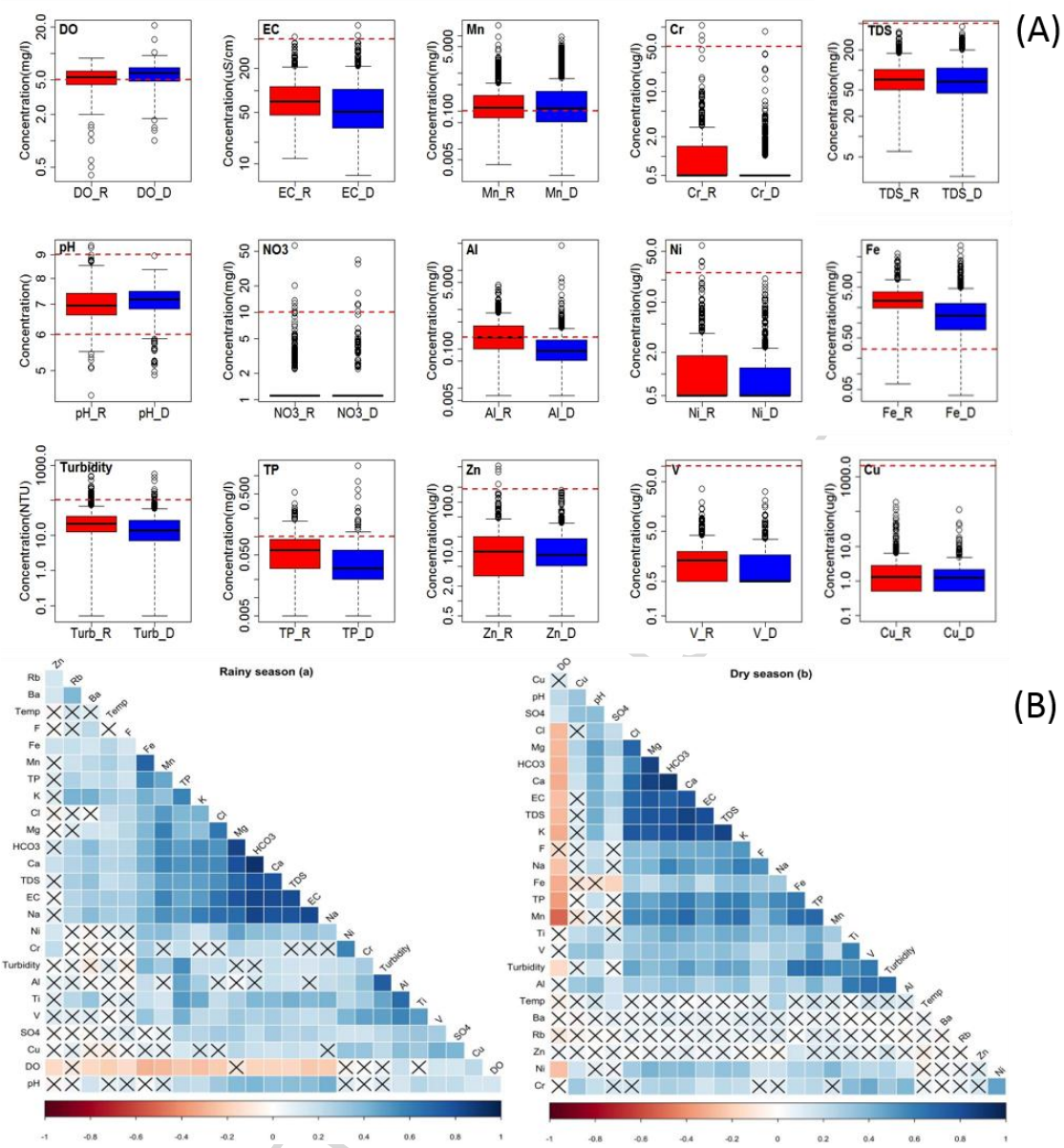

Fig. 3. (A) Boxplots of selective parameters in stream water of the Itacaiúnas river basin, obtained during rainy (-R; **red color**) and dry (-D; **blue color**) seasons. The box indicates approximately the 25th, 50th (median =black line) and 75th percentile; outliers (marked with points) are defined according to: (upper whisker, lower whisker) = (upper hinge, lower hinge) ± 1.5*hinge width. The traced red line indicate limits defined in CONAMA (2005); and **(B)** matrix of Spearman's correlation coefficient for physico-chemical parameters of stream waters collected in the rainy (a) and dry (b) periods from Itacaiunas basin.

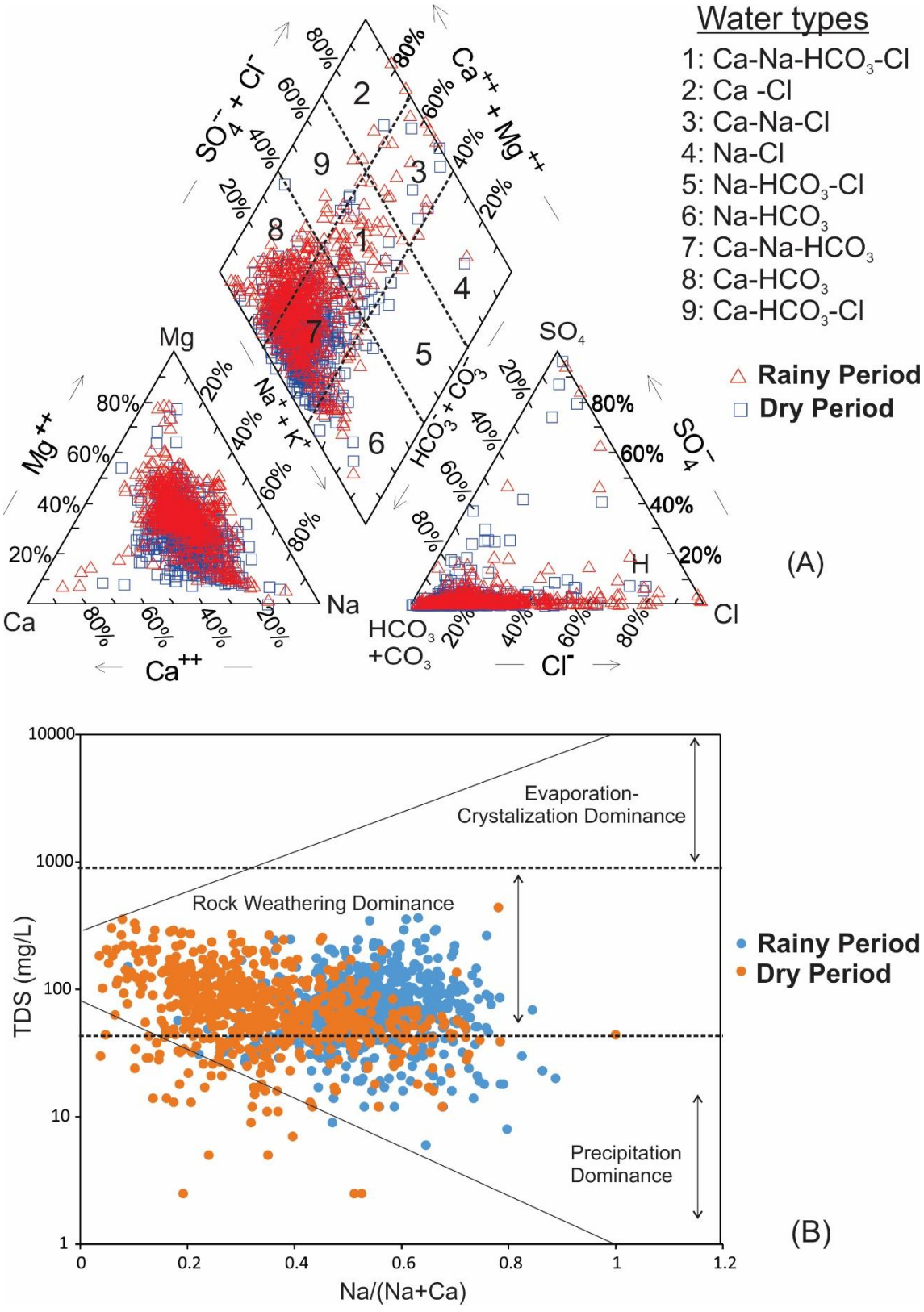

Fig. 4. (A) Piper diagram showing surface water type and **(B)** Gibbs plot showing the major process responsible for hydrogeochemistry of the Itacaiúnas basin in the dry and rainy periods.

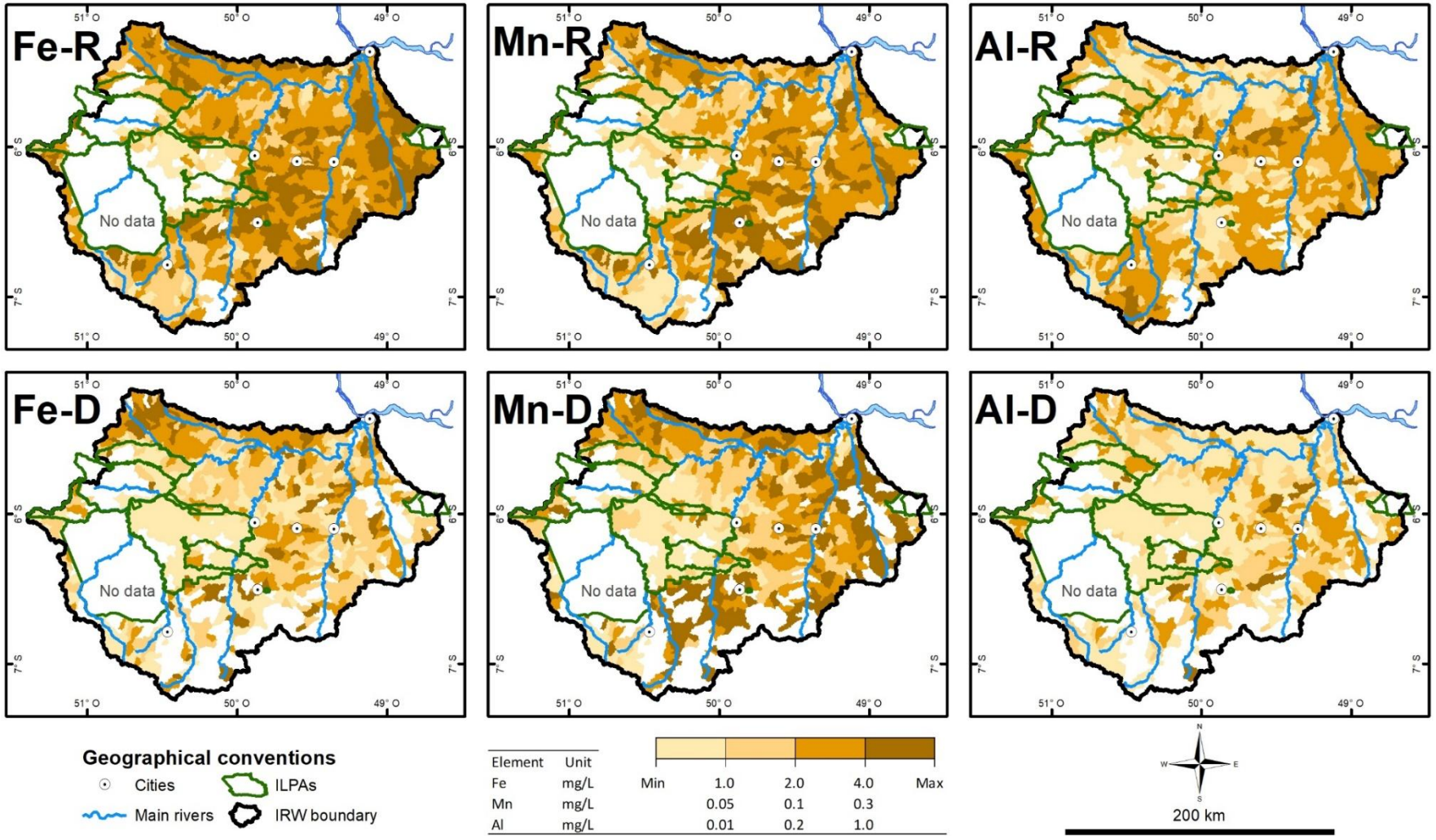

Continued.....

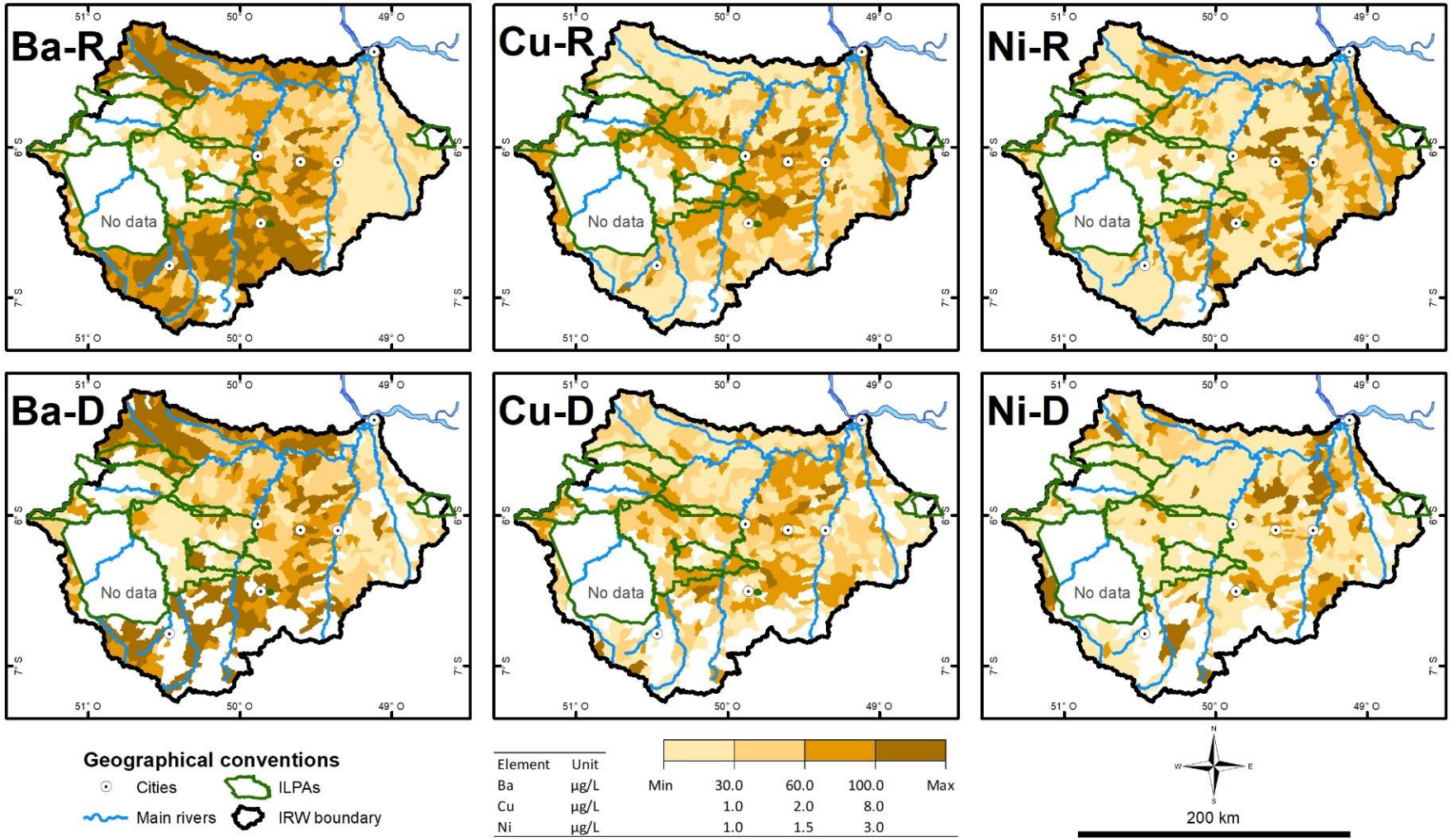

Fig. 5. Geochemical distribution of Fe, Mn, Al, Ba, Cu, Ni, and Cr in stream water of the Itacaiúnas River Basin. The samples were collected during rainy (-R) and dry (-D) seasons along 2017. Refer to Fig. 2 for the remarks applied, and to Table 2 for the detection limit.

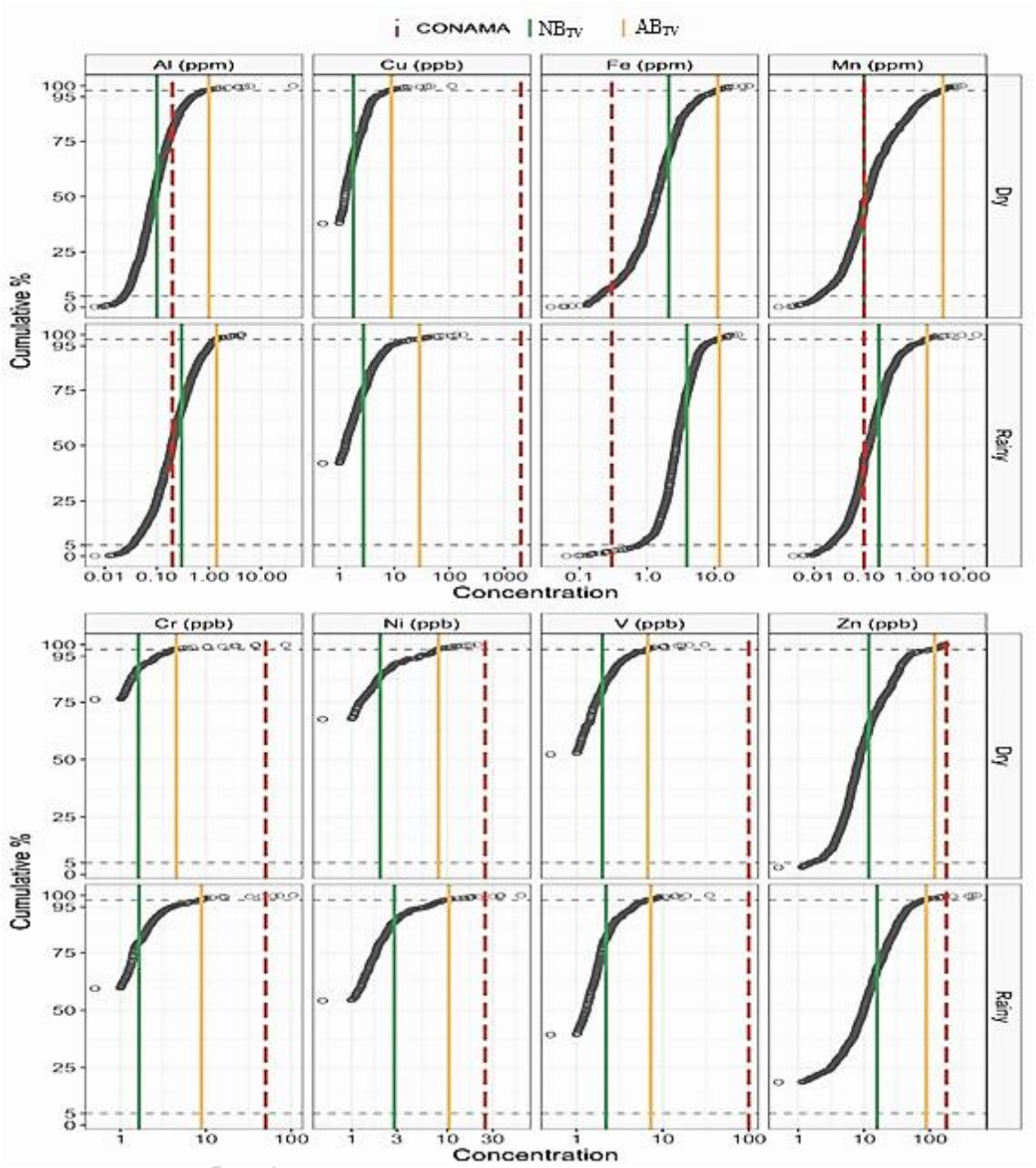

Fig. 6. Cumulative distribution of natural baseline (NB_{TV}) and ambient baseline threshold (AB_{TV}) levels of metals in the dry and rainy period. The vertical green line indicates NB_{TV}, pale-yellow for AB_{TV}, and red for CONAMA Class 2 limit.

Table 1: Statistical summary of water quality parameters in the Itacaiúnas River basin during rainy (_R) and dry (_D) seasons. n: number of samples; DL: detection limit; Min: minimum concentration; Max: maximum; M: 50th percentile of the data set, also known as median; SD: standard deviation; CV: coefficient of variation.

Parameter	n	Unit	DL	%<DL	Min	Max	Mean	M	SD	CV	Mean*	M*	SD*	CONAMA**
DO_R	720	mg/l	0.1	0.12	0.05	8.80	5.22	5.30	1.34	25.67	5.01	5.25	1.45	5
DO_D	638	mg/l	0.1	0	1.00	14.30	5.95	5.90	5.65	94.96	5.50	5.89	1.45	
pH_R	720		-	0	4.40	9.41	7.02	6.96	0.62	8.83	6.92	6.92	1.10	6-9
pH_D	638		-	0	4.88	8.96	7.11	7.17	0.54	7.59	7.08	7.24	1.07	
Temp_R	720	ºC	-	0	24.90	37.00	25.80	25.80	1.88	7.29	25.70	25.70	1.10	
Temp_D	638	ºC	-	0	27.70	32.50	25.48	25.40	2.51	9.85	25.12	25.12	1.12	
EC_R	720	µS/cm	1	0	12.00	534.00	90.09	71.00	66.52	73.84	72.44	70.79	1.91	
EC_D	638	µS/cm	1	0	7.00	752.00	81.62	51.00	81.74	100.15	56.23	51.29	2.29	
TDS_R	720	mg/l	5	0.12	6.00	364.00	81.85	71.00	48.81	59.63	69.18	70.79	1.78	
TDS_D	638	mg/l	5	0.5	2.50	440.00	83.86	66.50	58.67	69.96	66.07	66.07	2.04	
Turbidity_R	720	NTU	0.1	0.6	0.05	930.00	34.25	21.25	53.61	156.53	21.38	21.38	2.69	100
Turbidity_D	638	NTU	0.1	0.5	0.05	557.00	23.26	13.95	38.10	163.80	13.49	13.80	2.88	
F_R	720	mg/l	0.05	69.46	<0.05	9.00	0.08	<0.05	0.39	487.50	<0.05	0.03	2.09	1.4
F_D	638	mg/l	0.05	44.3	<0.05	12.70	0.09	0.06	0.50	555.56	0.05	0.06	2.19	
Cl_R	720	mg/l	0.5	0.37	<0.05	58.90	5.54	3.87	5.60	101.08	4.07	3.89	2.14	250
Cl_D	638	mg/l	0.5	0.5	0.25	112.00	7.99	4.50	10.60	132.67	5.13	4.47	2.45	
TP_R	720	mg/l	0.01	7.5	<0.01	0.53	0.07	0.06	0.05	71.43	0.05	0.06	2.34	
TP_D	638	mg/l	0.01	16.8	<0.01	1.41	0.05	0.03	0.08	160.00	0.03	0.03	2.69	
NO_3_R	720	mg/l	2.2	85	<2.2	57.50	1.62	<2.2	2.56	158.02	1.32	<2.2	1.62	10
NO_3_D	638	mg/l	2.2	89.3	<2.2	40.00	1.51	<2.2	2.38	157.62	1.26	<2.2	1.55	
SO_4_R	720	mg/l	0.5	55.5	<0.5	128.00	1.50	<0.5	7.10	473.33	0.51	<0.5	2.75	250
SO_4_D	638	mg/l	0.5	69	<0.5	121.00	1.11	<0.5	5.98	538.74	0.41	<0.5	2.51	
HCO_3_R	720	mg/l	-	2	0.10	250.56	47.78	39.94	33.85	70.85	37.15	39.81	2.24	
HCO_3_D	638	mg/l	-	3	0.38	234.38	44.14	32.06	37.33	84.57	30.90	32.36	2.51	
TH_R	720	mg/l	-	0	1.70	218.83	30.69	25.08	23.48	76.51	24.55	25.12	2.00	
TH_D	638	mg/l	-	0	1.32	207.06	33.32	22.89	30.07	90.25	23.44	22.91	2.34	
Ca_R	720	mg/l	0.001	0	0.15	36.20	6.32	5.19	4.52	71.52	5.01	5.25	2.04	
Ca_D	638	mg/l	0.001	0	<0.005	58.30	6.10	4.26	5.94	97.38	4.17	4.27	2.57	
Na_R	720	mg/l	0.001	0	0.71	61.90	7.59	6.01	6.06	79.84	5.89	6.03	2.04	
Na_D	638	mg/l	0.001	0	0.01	86.90	2.77	2.31	3.83	138.27	2.04	2.29	2.29	
Mg_R	720	mg/l	0.001	0	0.11	34.50	3.63	2.73	3.40	93.66	2.69	2.75	2.19	
Mg_D	638	mg/l	0.001	0	0.22	37.50	4.41	3.00	4.48	101.59	3.02	3.02	2.45	
K_R	720	mg/l	0.001	0.14	0.12	35.60	2.86	2.59	2.13	74.48	2.40	2.57	1.86	
K_D	638	mg/l	0.001	0	0.42	86.60	8.70	5.86	8.12	93.33	6.17	5.89	2.29	
Fe_R	720	mg/l	0.001	0	0.06	22.40	3.29	2.70	2.44	74.16	2.63	2.69	2.09	0.3[#]
Fe_D	638	mg/l	0.001	0	0.04	32.30	2.14	1.37	2.83	132.24	1.29	1.38	2.75	
Al_R	720	mg/l	0.001	0	0.01	4.26	0.33	0.20	0.44	133.33	0.19	0.19	2.82	0.2[#]
Al_D	638	mg/l	0.001	0	0.01	41.30	0.24	0.09	1.68	700.00	0.10	0.09	2.69	
Mn_R	720	mg/l	0.001	0	<0.001	18.00	0.29	0.12	0.86	296.55	0.13	0.13	3.09	0.1
Mn_D	638	mg/l	0.001	0.14	<0.001	9.14	0.42	0.12	0.89	211.90	0.13	0.12	4.37	
Cu_R	720	µg/l	1	42.3	<1	178.00	3.51	1.29	11.90	339.03	1.38	1.29	2.95	2[#]
Cu_D	638	µg/l	1	39.5	<1	112.00	2.06	1.27	5.36	260.19	1.23	1.26	2.34	
Ni_R	720	µg/l	1	56.3	<1	59.10	1.77	<1	3.72	210.17	1.00	<1	2.45	0.025
Ni_D	638	µg/l	1	68.98	<1	20.70	1.32	<1	2.12	160.61	0.81	<1	2.24	
Zn_R	720	µg/l	1	17	<1	517.00	17.38	9.82	35.01	201.44	6.92	9.77	4.68	0.18
Zn_D	638	µg/l	1	3.4	<1	170.00	16.35	8.48	23.27	142.32	9.33	8.51	2.88	
Cr_R	720	µg/l	1	61	<1	105.00	1.70	<1	5.81	341.76	0.89	<1	2.29	0.05
Cr_D	638	µg/l	1	77.9	<1	85.70	1.19	<1	4.27	358.82	0.69	<1	2.00	
Rb_R	720	µg/l	5	40.92	2.50	62.90	7.28	6.07	6.15	84.48	5.62	6.03	2.04	
Rb_D	638	µg/l	5	51	2.50	21.30	5.44	2.50	3.63	66.73	4.47	2.51	1.86	
Ti_R	720	µg/l	1	7	<1	94.60	8.08	4.83	10.48	129.70	4.79	4.79	2.75	
Ti_D	638	µg/l	1	3.5	<1	68.90	5.10	3.63	5.38	105.49	3.89	3.63	2.00	
Cd_R	720	µg/l	1	99	<1	10.00	0.52	<1	0.41	78.85	<1	<1	1.17	0.001
Cd_D	638	µg/l	1	100	<1	0.50	<1	<1	<1	<1	<1	<1	1.00	
As_R	720	µg/l	1	95.5	<1	4.37	0.57	<1	0.37	64.91	0.54	<1	1.35	0.01
As_D	638	µg/l	1	95.2	<1	3.72	0.57	<1	0.35	61.40	0.54	<1	1.32	
Ba_R	720	µg/l	1	0	4.09	412.00	72.87	60.65	55.17	75.71	54.95	60.26	2.19	0.7
Ba_D	638	µg/l	1	0.14	0.13	967.00	67.14	44.50	77.27	115.09	38.90	44.67	3.16	
B_R	720	µg/l	1	38	<1	209.00	4.49	2.50	10.10	224.94	2.00	2.51	3.55	
B_D	638	µg/l	1	67.5	<1	499.00	3.15	<1	20.48	650.16	1.02	<1	3.09	
Pb_R	720	µg/l	1	84.6	<1	23.50	0.76	<1	1.15	151.32	0.62	<1	1.66	0.01
Pb_D	638	µg/l	1	93.5	<1	7.07	0.59	<1	0.49	83.05	0.54	<1	1.38	
Se_R	720	µg/l	1	99	<1	3.90	0.52	<1	0.19	36.54	<1	<1	1.15	
Se_D	638	µg/l	1	85.8	<1	9.25	0.72	<1	0.75	104.17	0.60	<1	1.62	
V_R	720	µg/l	1	42	<1	35.00	1.66	1.31	2.10	126.51	1.17	1.32	2.19	0.1
V_D	638	µg/l	1	55.84	<1	31.10	1.46	<1	2.12	145.21	0.98	<1	2.24	
Sn_R	720	µg/l	1	49.8	<1	22.40	1.95	<1	2.59	132.82	1.12	<1	2.63	
Sn_D	638	µg/l	1	22	<1	25.30	2.68	2.19	2.75	102.61	1.86	2.19	2.34	
Sr_R	720	µg/l	1	0	2.28	507.00	64.09	44.45	65.60	102.36	42.66	44.67	2.57	
Sr_D	638	µg/l	1	0.7	<1	841.00	62.46	38.35	79.65	127.52	36.31	38.02	2.88	

Co_R	720	µg/l	1	65	<1	33.80	1.26	<1	1.97	156.35	0.83	<1	2.14
Co_D	638	µg/l	1	64	<1	29.90	1.32	<1	2.12	160.61	0.85	<1	2.19

*: parameters calculated based on log-transformed data; **: Brazilian CONAMA Resolution 357/2005 of Class 2 limits; #: values adopted from WHO (1998) drinking water quality; TH: total hardness; -: data not available.

Table 2. Geochemical baseline threshold values (upper limit) obtained from various statistical methods [Median + 2 MAD, Tukey's inner fences (TIF), cumulative frequency (CF) distribution diagrams, iterative 2σ technique (I2σ), calculated distribution function (DF) and percentile (Q75, Q95, G98] and Class-I and Class-II levels for 18 elements in stream water of the Itacaiúnas River basin during the rainy (_R) and dry (_D) seasons of 2017.

Parameter	Unit	n	%<DL	Q75	CF	I2σ	DF	MAD	Q95	Q98	TIF	CONAMA*
Fe_R	mg/l	720	0	3.98	5.60	**3.90**	5.00	7.76	7.08	***11.82***	11.61	0.3#
Fe_D	mg/l	638	0	2.40	3.10	**2.10**	2.90	7.59	6.46	***11.22***	13.96	
Al_R	mg/l	720	0	0.39	0.50	**0.30**	0.40	1.48	1.05	***1.41***	2.99	0.2#
Al_D	mg/l	638	0	0.17	0.19	**0.10**	0.20	0.49	0.48	***1.00***	0.97	
Mn_R	mg/l	720	0	0.26	0.31	**0.20**	0.30	0.91	0.89	***1.83***	1.91	0.1
Mn_D	mg/l	638	0.14	0.32	0.30	**0.10**	0.30	1.55	1.78	***3.80***	4.95	
Cu_R	µg/l	720	42.3	2.75	3.80	-	**2.80**	21.38	8.51	***28.63***	35.48	2
Cu_D	µg/l	638	39.5	2.19	2.51	**1.80**	2.60	19.95	4.57	***8.82***	19.95	
Ni_R	µg/l	720	56.3	1.82	**2.80**	-	-	-	6.03	***10.46***	12.59	0.025
Ni_D	µg/l	638	68.98	1.23	**1.99**	-	-	-	5.25	***8.10***	4.73	
Zn_R	µg/l	720	17	19.95	32.00	**15.80**	23.60	128.82	50.12	***88.12***	316.23	0.18
Zn_D	µg/l	638	3.4	18.20	14.00	**11.80**	16.90	51.29	47.86	***118.44***	121.62	
Cr_R	µg/l	720	61	1.45	**1.65**	-	-	-	3.98	***8.88***	7.08	0.05
Cr_D	µg/l	638	77.9	-	**1.62**	-	-	-	2.69	***4.50***	-	
Ti_R	µg/l	720	7	8.91	8.30	**7.20**	9.90	27.54	26.30	***44.81***	53.70	
Ti_D	µg/l	638	3.5	5.62	6	**4.20**	6.40	12.02	13.49	***20.93***	18.20	
V_R	µg/l	720	42	1.95	2.08	**2.20**	2.70	14.45	4.68	***7.27***	14.96	0.1
V_D	µg/l	638	55.84	1.70	**1.90**	-	-	-	4.07	***6.71***	10.59	
Co_R	µg/l	720	65	1.38	**1.99**	-	-	-	4.17	***6.71***	6.31	
Co_D	µg/l	638	64	1.35	**1.47**	-	-	-	4.17	***8.06***	5.96	
Ba_R	µg/l	720	0	100.00	91.00	**119.00**	122.00	302.00	169.82	***231.58***	524.81	0.7
Ba_D	µg/l	638	0.14	89.13	100.00	**60.20**	97.70	371.54	194.98	***291.44***	841.40	
Rb_R	µg/l	720	40.92	9.33	7.94	**9.50**	12.30	63.10	18.62	***24.32***	66.83	
Rb_D	µg/l	638	51	7.59	6.76	**7.70**	-	2.51	12.02	***14.22***	39.81	
Sn_R	µg/l	720	49.8	2.57	**3.16**	-	-	-	6.46	***10.97***	29.85	
Sn_D	µg/l	638	22	3.16	3.98	**3.70**	4.60	8.32	6.61	***13.22***	13.96	
Sr_R	µg/l	720	0	75.86	89.00	**67.30**	91.50	257.04	194.98	***274.58***	426.58	
Sr_D	µg/l	638	0.7	67.61	66.00	**60.50**	80.60	229.09	218.78	***344.18***	421.70	
B_R	µg/l	720	38	5.75	**11.00**	-	6.10	138.04	13.18	***18.35***	223.87	
B_D	µg/l	638	67.5	2.29	**10.10**	-	-	-	9.12	***13.92***	22.39	
Pb_R	µg/l	720	84.6	-	-	-	-	-	**1.82**	***2.80***	-	0.01
Pb_D	µg/l	638	93.5	-	-	-	-	-	**1.10**	***1.81***	-	
As_R	µg/l	720	95.5	-		-	-	-	-	**1.77**	-	0.01
As_D	µg/l	638	95.2	-		-	-	-	-	**1.93**	-	
Se_R	µg/l	720	99	-	-	-	-	-	-	-	-	
Se_D	µg/l	638	85.8	-	-	-	-	-	**1.95**	3.16	-	

Bold: natural baseline threshold values (NB_{TVs}); ***Italic***: ambient threshold values (AB_{TVs}); *: Brazilian CONAMA Resolution 357/2005 of Class 2 limits; #: values adopted from WHO (1998) drinking water quality; -: data not available.

Highlights

- First detailed high density hydrogeochemical survey was carried out in Itacaiúnas basin;
- We estimated the natural baseline levels (NaBT) and ambient baseline level (AmBT);
- We employed a concept of unmineralized (UnB) & mineralized (MiB) baseline levels;
- High AmBT of Fe and Mn in waters are related to local land use change activities;
- The MiB level of Cu is highly influenced by the hydrothermal mineralized copper belts;